LARGE TIME ASYMPTOTIC BEHAVIOR OF GRAIN BOUNDARIES MOTION WITH DYNAMIC LATTICE MISORIENTATIONS AND WITH TRIPLE JUNCTIONS DRAG*

YEKATERINA EPSHTEYN†, CHUN LIU‡, AND MASASHI MIZUNO§

Abstract. Many technologically useful materials are polycrystals composed of a myriad of small monocrystalline grains separated by grain boundaries. Dynamics of grain boundaries play an essential role in defining the material's properties across multiple scales. In this work, we study the large-time asymptotic behavior of the model for the motion of grain boundaries with the dynamic lattice misorientations and the triple junctions drag.

Keywords. Grain growth; grain boundary network; texture development; lattice misorientation; triple junction drag; energetic variational approach; geometric evolution equations; large-time asymptotics.

AMS subject classifications. 74N15; 35R37; 53C44; 49Q20.

1. Introduction

Many technologically useful materials are polycrystals composed of a myriad of small monocrystalline grains separated by grain boundaries. Dynamics of grain boundaries play an essential role in defining the material's properties across multiple scales. Experimental and computational studies give useful insight into the geometric features and the crystallography of the grain boundary network in polycrystalline microstructures.

The focus of this work is on the large-time evolution of a planar grain boundary network. A classical model for the motion of grain boundaries in polycrystalline materials is the growth by curvature, as the local evolution law for the grain boundaries, due to Mullins and Herring [18, 30, 31], and see also work on mean curvature flow, e.g., [10, 11, 16, 24]. In addition, to have a well-posed model for the evolution of the grain boundary network, one has to impose a separate condition at the triple junctions where three grain boundaries meet [20]. A conventional choice is the Herring condition which is the natural boundary condition at the triple points for the grain boundary network at equilibrium, [8,9,19,20], and references therein. There are several analytical studies about grain boundary motion by mean curvature with the Herring condition at the triple junctions, see for instance [1–6,17,20,22,23,25–28], as well as computational work, [2,5,12–14,21,33].

A standard assumption in the theory and simulations of the grain growth is the evolution of the grain boundaries/interfaces themselves and not the dynamics of the triple junctions. However, recent experimental work indicates that the motion of the triple junctions together with the anisotropy of the grain interfaces can have a significant effect on the resulting grain growth [6], see also work on molecular dynamics simulation [33,34] and a recent work on dynamics of line defects [32,35,36]. The current work is a

†Department of Mathematics, The University of Utah, Salt Lake City, UT 84112, USA (epshteyn@math.utah.edu).

‡Department of Applied Mathematics, Illinois Institute of Technology, Chicago, IL 60616, USA (cliu124@iit.edu).

§Department of Mathematics, College of Science and Technology, Nihon University, Tokyo 101-8308, Japan (mizuno@math.cst.nihon-u.ac.jp).

continuation of our previous work [15], where we proposed a new model for the evolution of planar grain boundaries, which takes into account dynamic lattice misorientations (evolving anisotropy of grain boundaries) and the mobility of the triple junctions. The goal here is to analyze the large-time asymptotic behavior of the model proposed in [15].

The paper is organized as follows. In Sections 2-3, we discuss important details and properties of the model for the grain boundary motion. In Sections 4-5, we present the main results of this paper, the global existence (Theorem 4.1), and the large-time asymptotic behavior of the considered model under the assumption of a single triple junction (Theorem 5.1). In Section 6, we discuss the extension of the theory to the grain boundary network with multiple junctions, under the assumption of no critical/disappearance events and around the energy minimizing state. Finally, in Section 7, we present several numerical experiments to illustrate the effect of the dynamic orientations/misorientations (grains "rotations") and the effect of the mobility of the triple junctions on the grain growth.

2. Review of the model

In this article we consider the large-time asymptotic behavior of the model for the evolution of the planar grain boundary network with the dynamic lattice misorientations and the triple junctions drag. Thus, in this section for the reader's convenience, we first review the model which was originally proposed in [15], and then, briefly preview main results of the current work.

Let us first recall the system for a single triple junction which was derived in [15]. The total grain boundary energy for such a model is

$$\sum_{j=1}^{3} \sigma(\Delta^{(j)}\alpha)|\Gamma_t^{(j)}|. \tag{2.1}$$

Here, $\sigma : \mathbb{R} \to \mathbb{R}$ is a given surface tension, $\alpha^{(j)} = \alpha^{(j)}(t) : [0,\infty) \to \mathbb{R}$ are time-dependent orientations of the grains, $\theta = \Delta^{(j)}\alpha := \alpha^{(j-1)} - \alpha^{(j)}$ is a lattice misorientation of the grain boundary $\Gamma_t^{(j)}$, and $|\Gamma_t^{(j)}|$ is the length of $\Gamma_t^{(j)}$. As a result of applying the maximal dissipation principle, in [15], one can obtain the following model,

$$\begin{cases} v_n^{(j)} = \mu\sigma(\Delta^{(j)}\alpha)\kappa^{(j)}, \quad \text{on } \Gamma_t^{(j)}, \ t>0, \quad j=1,2,3, \\[2mm] \dfrac{d\alpha^{(j)}}{dt} = -\gamma\Big(\sigma_\theta(\Delta^{(j+1)}\alpha)|\Gamma_t^{(j+1)}| - \sigma_\theta(\Delta^{(j)}\alpha)|\Gamma_t^{(j)}|\Big), \quad j=1,2,3, \\[2mm] \dfrac{d\boldsymbol{a}}{dt}(t) = \eta\sum_{k=1}^{3}\sigma(\Delta^{(k)}\alpha)\dfrac{\boldsymbol{b}^{(k)}(0,t)}{|\boldsymbol{b}^{(k)}(0,t)|}, \quad t>0, \\[2mm] \Gamma_t^{(j)} : \boldsymbol{\xi}^{(j)}(s,t), \quad 0 \le s \le 1, \quad t>0, \quad j=1,2,3, \\[2mm] \boldsymbol{a}(t) = \boldsymbol{\xi}^{(1)}(0,t) = \boldsymbol{\xi}^{(2)}(0,t) = \boldsymbol{\xi}^{(3)}(0,t), \quad \text{and} \quad \boldsymbol{\xi}^{(j)}(1,t) = \boldsymbol{x}^{(j)}, \quad j=1,2,3. \end{cases} \tag{2.2}$$

In (2.2), $v_n^{(j)}$, $\kappa^{(j)}$, and $\boldsymbol{b}^{(j)} = \boldsymbol{\xi}_s^{(j)}$ denote a normal velocity, a curvature and a tangent vector of the grain boundary $\Gamma_t^{(j)}$, respectively. Note that s is not an arc length parameter of $\Gamma_t^{(j)}$, namely, $\boldsymbol{b}^{(j)}$ is *not* necessarily a unit tangent vector. The vector $\boldsymbol{a} = \boldsymbol{a}(t) : [0,\infty) \to \mathbb{R}^2$ denotes a position of the triple junction, $\boldsymbol{x}^{(j)}$ is a position of the end point of the grain boundary. The three independent relaxation time scales $\mu, \gamma, \eta > 0$ (length, misorientation and position of the triple junction) are considered as positive constants. Further, we assume in (2.2), $\alpha^{(0)} = \alpha^{(3)}$, $\alpha^{(4)} = \alpha^{(1)}$ and $\boldsymbol{b}^{(4)} = \boldsymbol{b}^{(1)}$, for simplicity. We also use notation $|\cdot|$ for a standard Euclidean vector norm. The complete
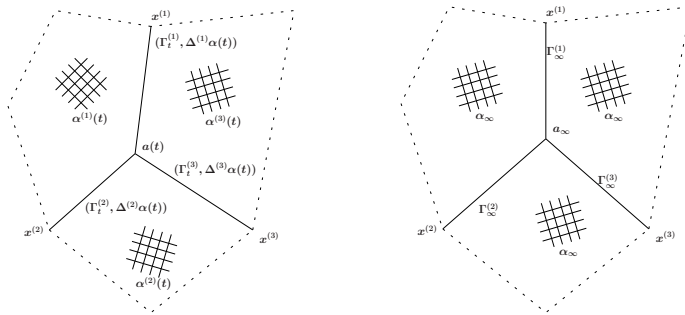
FIG. 2.1. *The left figure illustrates the model* (2.3)*, where we isolate the effect of the misorientations and mobility of the triple junction on the motion of the grain boundaries. The right figure illustrates the model of the equilibrium state* (2.9) *with no misorientation effect.*

details about model (2.2) can be found in the earlier work [15, Section 2]. Next, in [15], we relaxed the curvature effect, by taking the limit $\mu \to \infty$, and obtained the reduced model (see Figure 2.1),

$$\begin{cases} \dfrac{d\alpha^{(j)}}{dt} = -\gamma\Big(\sigma_\theta(\Delta^{(j+1)}\alpha)|\boldsymbol{b}^{(j+1)}| - \sigma_\theta(\Delta^{(j)}\alpha)|\boldsymbol{b}^{(j)}|\Big), \quad j = 1, 2, 3, \\ \dfrac{d\boldsymbol{a}}{dt}(t) = \eta \sum_{j=1}^{3} \sigma(\Delta^{(j)}\alpha)\dfrac{\boldsymbol{b}^{(j)}}{|\boldsymbol{b}^{(j)}|}, \quad t > 0, \\ \boldsymbol{a}(t) + \boldsymbol{b}^{(j)}(t) = \boldsymbol{x}^{(j)}, \quad j = 1, 2, 3. \end{cases} \tag{2.3}$$

In (2.3), we consider $\boldsymbol{b}^{(j)}(t)$ as a grain boundary. Note that, the system of equations (2.3) can also be derived from the energetic variational principle for the total grain boundary energy (2.1) (with $|\Gamma_t^{(j)}|$ replaced by $|\boldsymbol{b}^{(j)}|$).

Hereafter, we assume the following three conditions for the surface tension σ. First, we assume σ is C^3, positive and is minimized at 0, namely,

$$\sigma(\theta) \geq \sigma(0) > 0, \tag{2.4}$$

for $\theta \in \mathbb{R}$. Second, we assume convexity, for all $\theta \in \mathbb{R}$,

$$\sigma_\theta(\theta)\theta \geq 0, \qquad \text{and} \quad \sigma_{\theta\theta}(0) > 0. \tag{2.5}$$

Furthermore, we assume,

$$\sigma_\theta(\theta) = 0 \text{ if and only if } \theta = 0. \tag{2.6}$$

REMARK 2.1.   Note, it is enough to assume $\sigma_{\theta\theta}(0) > 0$ instead of (2.5) if $\Delta^{(j)}\alpha$ are sufficiently small. Indeed, if C^2 function σ satisfies $\sigma_{\theta\theta}(0) > 0$ and $\sigma(\theta) \geq \sigma(0)$ for $\theta \in \mathbb{R}$, then $\sigma_\theta(\theta)\theta \geq 0$ is satisfied for sufficiently small $|\theta|$. Note that, the convexity assumption (2.5) was not used for the local existence result, see [15] (or see Proposition 3.1 below). Further, we can also show the maximum principle (Proposition 3.3) without global convexity assumption $\sigma_\theta(\theta)\theta \geq 0$ in (2.5), if the initial orientations $\alpha_0^{(j)}$ are sufficiently small.

Next, to preview the ideas of main results of this work, consider the equilibrium state of the grain boundary energy (2.1), namely,

$$
\begin{cases}
0 = -\Big(\sigma_\theta(\Delta^{(j+1)}\alpha_\infty)|\boldsymbol{b}_\infty^{(j+1)}| - \sigma_\theta(\Delta^{(j)}\alpha_\infty)|\boldsymbol{b}_\infty^{(j)}|\Big), \\
\boldsymbol{0} = \sum_{j=1}^{3} \sigma(\Delta^{(j)}\alpha_\infty)\frac{\boldsymbol{b}_\infty^{(j)}}{|\boldsymbol{b}_\infty^{(j)}|}, \\
\boldsymbol{a}_\infty = \boldsymbol{x}^{(1)} - \boldsymbol{b}_\infty^{(1)} = \boldsymbol{x}^{(2)} - \boldsymbol{b}_\infty^{(2)} = \boldsymbol{x}^{(3)} - \boldsymbol{b}_\infty^{(3)}.
\end{cases}
\tag{2.7}
$$

Assume, for each $i = 1, 2, 3$,

$$
\left| \sum_{j=1, j\neq i}^{3} \frac{\boldsymbol{x}^{(j)} - \boldsymbol{x}^{(i)}}{|\boldsymbol{x}^{(j)} - \boldsymbol{x}^{(i)}|} \right| > 1.
\tag{2.8}
$$

The assumption (2.8) implies that fixed points $\boldsymbol{x}^{(1)}, \boldsymbol{x}^{(2)}$ and $\boldsymbol{x}^{(3)}$ can not belong to the single line. Furthermore, (2.8) is equivalent to the condition that in the triangle with vertices $\boldsymbol{x}^{(1)}\boldsymbol{x}^{(2)}\boldsymbol{x}^{(3)}$, all three angles are less than $\frac{2\pi}{3}$. Next, from the assumption (2.8), (2.5)-(2.6), associated equilibrium system (2.7) becomes,

$$
\begin{cases}
\sum_{j=1}^{3} \frac{\boldsymbol{b}_\infty^{(j)}}{|\boldsymbol{b}_\infty^{(j)}|} = \boldsymbol{0}, \\
\boldsymbol{a}_\infty + \boldsymbol{b}_\infty^{(j)} = \boldsymbol{x}^{(j)}, \quad j = 1, 2, 3.
\end{cases}
\tag{2.9}
$$

In fact, assumptions (2.5)-(2.6) imply $\alpha_\infty^{(1)} = \alpha_\infty^{(3)} = \alpha_\infty^{(3)}$, hence $\Delta^{(j)}\alpha_\infty = 0$ for $j = 1, 2, 3$. We later discuss the property of the equilibrium solution of (2.7) in Proposition 5.1.

The main result of this work is the local exponential stability for the solution of the equilibrium state (2.9), Theorem 5.1. That is, if the initial misorientations are sufficiently small and the position of the initial triple junction is sufficiently close to the equilibrium state of the position of the triple junction, then, the solution of (2.3) exists globally in time and it exponentially converges to the equilibrium solution of (2.9). Our strategy of the proof here is to show a priori estimate for the position of the triple junction, and then study the linearized problem of (2.3) around the equilibrium state. With the aid of the assumption (2.8), the equilibrium state system (2.9) is uniquely solvable. Moreover, the equilibrium state is also the energy minimizing state. Thus, we can obtain a priori estimate for the position of the triple junction and a full convergence result for large-time asymptotics of the solution. Again thanks to (2.8), the linearized operator of (2.3) is degenerate if and only if, there are no misorientation effects, that is, all $\alpha^{(j)}$ are the same. This allows us to deduce the exponential stability for the equilibrium state.

Moreover, we consider large-time asymptotic behavior of the grain boundary network. In general, the uniqueness for the equilibrium state is not known, and there might be critical events (disappearance of the grains, grain boundaries, etc. [2–5]). We study the large-time asymptotics of the grain boundary network in Section 6 under the assumption of no critical events and around the energy minimizing state. We discuss global existence and large-time asymptotic behavior of the grain boundary network in Section 6.

3. Properties of the local solution

In this section, for the reader's convenience, we review some known results, as well as established additional properties for the system, defined in (2.3). In particular, we review local existence and a priori estimates results for the model (2.3). More details can be found in [15].

First, using the same argument as in [15], one can show the local-in-time existence of the triple junction and the estimates of the maximal existence time, under assumption of more general relaxation time constants, $\gamma, \eta > 0$.

PROPOSITION 3.1 (Local existence [15, Theorem 4.1]).   *Let $\boldsymbol{x}^{(1)}, \boldsymbol{x}^{(2)}, \boldsymbol{x}^{(3)} \in \mathbb{R}^2$, $\boldsymbol{a}_0 \in \mathbb{R}^2$, and $\boldsymbol{\alpha}_0 \in \mathbb{R}^3$ be given initial data. Assume the conditions (2.4) and (2.8) for $i = 1, 2, 3$, and let $\boldsymbol{a}_\infty$ be a solution of (2.9). Further, assume that for all $j = 1, 2, 3$,*

$$|\boldsymbol{a}_0 - \boldsymbol{a}_\infty| < \frac{1}{2}|\boldsymbol{b}_\infty^{(j)}|. \tag{3.1}$$

Then, there exists a local-in-time solution $(\boldsymbol{\alpha}, \boldsymbol{a})$ of (2.3) on $[0, T_{max})$, such that

$$|\boldsymbol{a}(t) - \boldsymbol{a}_\infty| < |\boldsymbol{b}_\infty^{(j)}| \quad \text{for all} \quad j = 1, 2, 3, \text{ and } 0 \leq t < T_{max}. \tag{3.2}$$

Furthermore, the maximal existence time T_{max} of the solution is estimated by

$$T_{max} \geq \min \left\{ \frac{|\boldsymbol{\alpha}_0|}{4\gamma(M_1 + 8M_2|\boldsymbol{\alpha}_0|)\sum_{j=1}^3 |\boldsymbol{b}_\infty^{(j)}|}, \frac{|\boldsymbol{a}_0 - \boldsymbol{a}_\infty|}{3\eta M_0}, \right.$$
$$\left. \frac{1}{12\gamma M_1}, \frac{1}{8\eta M_0 \sum_{j=1}^3 \frac{1}{|\boldsymbol{b}_\infty^{(j)}| - 2|\boldsymbol{a}_0 - \boldsymbol{a}_\infty|}} \right\} \tag{3.3}$$

where

$$M_0 := \sup_{|\theta| \leq 4|\boldsymbol{\alpha}_0|} |\sigma(\theta)|, \quad M_1 := \sup_{|\theta| \leq 4|\boldsymbol{\alpha}_0|} |\sigma_\theta(\theta)|, \quad M_2 := \sup_{|\theta_1|, |\theta_2| \leq 4|\boldsymbol{\alpha}_0|} \frac{|\sigma_\theta(\theta_1) - \sigma_\theta(\theta_2)|}{|\theta_1 - \theta_2|}.$$

To show Proposition 3.1, the contraction mapping principle is employed [15]. Note that, the assumption (3.2) guarantees that the point vector $\boldsymbol{a}$ does not coincide with the Dirichlet point $\boldsymbol{x}^{(j)}$, and stays as the triple junction. Note also, if one can obtain a priori bounds for $|\boldsymbol{\alpha}|$ and $|\boldsymbol{a} - \boldsymbol{a}_\infty|$, then from (3.3) the solution given by Proposition 3.1 can be extended globally in time.

Next we review some a priori estimates for (2.3). Since our problem (2.3) ensures the energy dissipation principle, one can obtain,

PROPOSITION 3.2 (Energy dissipation [15, Proposition 5.1]).   *Let $(\boldsymbol{\alpha}, \boldsymbol{a})$ be a solution of (2.3) on $0 \leq t \leq T$, and let $E(t)$, given by (2.1), be the total grain boundary energy of the system. Then, for all $0 < t \leq T$,*

$$E(t) + \frac{1}{\gamma} \int_0^t \left| \frac{d\boldsymbol{\alpha}}{dt}(\tau) \right|^2 d\tau + \frac{1}{\eta} \int_0^t \left| \frac{d\boldsymbol{a}}{dt}(\tau) \right|^2 d\tau = E(0). \tag{3.4}$$

The estimate (3.4) is obtained by taking the derivative of the energy $E(t)$ and using the system (2.3).

We also have a maximum principle for the orientation $\alpha^{(j)}$,

PROPOSITION 3.3 (Maximum principle [15, Proposition 5.1]). *Let $(\boldsymbol{\alpha}, \boldsymbol{a})$ be a solution of* (2.3) *on* $0 \leq t \leq T$. *Then, for all* $0 < t \leq T$,

$$|\boldsymbol{\alpha}(t)|^2 \leq |\boldsymbol{\alpha}_0|^2. \tag{3.5}$$

The estimate (3.5) can be obtained by multiplying the equation of $\alpha^{(j)}$ in (2.3) by $\alpha^{(j)}$ and integrating in time. Since, the right-hand side of the first equation in (2.3) is non-positive definite for all $t > 0$, the maximum principle for the orientations $\boldsymbol{\alpha}$ holds.

In addition, since $\frac{d}{dt}(\alpha^{(1)} + \alpha^{(2)} + \alpha^{(3)}) = 0$, we obtain that the sum of the orientations is preserved, namely,

LEMMA 3.1 (Preserving total orientations).   *Let $(\boldsymbol{\alpha}, \boldsymbol{a})$ be a solution of* (2.3) *on* $0 \leq t \leq T$. *Then, for all* $0 < t \leq T$,

$$\alpha^{(1)}(t) + \alpha^{(2)}(t) + \alpha^{(3)}(t) = \alpha_0^{(1)} + \alpha_0^{(2)} + \alpha_0^{(3)}. \tag{3.6}$$

Above, we discussed some known results about the system (2.3) (cf. [15]). In the current work, we employ these results to show the existence of the global solution, and obtain the large-time asymptotic behavior of the solution to (2.3).

4. Global existence

In this section, existence theory for a global-in-time solution of (2.3) is presented. As mentioned after the Proposition 3.1 in Section 3, in order to show the global existence in time of (2.3), we need to derive a priori estimates for $|\boldsymbol{\alpha}|$ and $|\boldsymbol{a} - \boldsymbol{a}_\infty|$. We already have a priori estimates for $|\boldsymbol{\alpha}|$, see Proposition 3.3 (the maximum principle). Therefore, the main objectives of this section are to obtain a priori estimates for $|\boldsymbol{a} - \boldsymbol{a}_\infty|$, Lemma 4.1, and then show the global existence result, Theorem 4.1.

Define,

$$C_1 := \inf\left\{\sum_{j=1}^{3} |\boldsymbol{x}^{(j)} - \boldsymbol{a}| : \text{There exists } j = 1, 2, 3 \text{ such that } |\boldsymbol{a} - \boldsymbol{a}_\infty| \geq \frac{1}{2}|\boldsymbol{b}_\infty^{(j)}|\right\}. \tag{4.1}$$

Since $\boldsymbol{a}_\infty$ is the unique minimizer of

$$f(\boldsymbol{a}) = \sum_{j=1}^{3} |\boldsymbol{x}^{(j)} - \boldsymbol{a}|, \quad \boldsymbol{a} \in \mathbb{R}^2 \tag{4.2}$$

and $f : \mathbb{R}^2 \to \mathbb{R}$ is continuous, we have,

$$0 < \sum_{j=1}^{3} |\boldsymbol{b}_\infty^{(j)}| = f(\boldsymbol{a}_\infty) < C_1. \tag{4.3}$$

Next lemma gives a priori estimate for the triple junction $\boldsymbol{a}$.

LEMMA 4.1 (Boundedness of the triple junction).   *Assume that an initial data $(\boldsymbol{\alpha}_0, \boldsymbol{a}_0)$ satisfies,*

$$E(0) = \sum_{j=1}^{3} \sigma(\Delta^{(j)}\alpha_0)|\boldsymbol{a}_0 - \boldsymbol{x}^{(j)}| < \sigma(0)C_1. \tag{4.4}$$

Let $(\boldsymbol{\alpha},\boldsymbol{a})$ be a solution of (2.3) *on* $0 \le t \le T$*. Then, we have that,*

$$|\boldsymbol{a}(t) - \boldsymbol{a}_\infty| < \frac{1}{2}|\boldsymbol{b}_\infty^{(j)}| = \frac{1}{2}|\boldsymbol{a}_\infty - \boldsymbol{x}^{(j)}| \tag{4.5}$$

for $j = 1, 2, 3$*, and for any* $0 \le t \le T$*.*

Proof. Assume, there is $0 \le t_1 \le T$ and $j = 1, 2, 3$, such that, $|\boldsymbol{a}(t_1) - \boldsymbol{a}_\infty| \ge \frac{1}{2}|\boldsymbol{b}_\infty^{(j)}|$. Then (2.4), (4.1) and Proposition 3.2 (energy dissipation) lead,

$$C_1 \le \sum_{j=1}^{3} |\boldsymbol{a}(t_1) - \boldsymbol{x}^{(j)}| = \sum_{j=1}^{3} |\boldsymbol{b}^{(j)}(t_1)| \le \frac{1}{\sigma(0)} \sum_{j=1}^{3} \sigma(\Delta^{(j)}\alpha_0)|\boldsymbol{a}_0 - \boldsymbol{x}^{(j)}| = \frac{1}{\sigma(0)} E(0),$$

which contradicts (4.4). □

REMARK 4.1. Note, if we assume (4.4), then we have,

$$\sum_{j=1}^{3} |\boldsymbol{a}_0 - \boldsymbol{x}^{(j)}| \le \frac{1}{\sigma(0)} \sum_{j=1}^{3} \sigma(\Delta^{(j)}\alpha_0)|\boldsymbol{a}_0 - \boldsymbol{x}^{(j)}| < C_1,$$

thus, $|\boldsymbol{a}_0 - \boldsymbol{a}_\infty| < |\boldsymbol{b}_\infty^{(j)}|/2$ for all $j = 1, 2, 3$. Hence, the assumption (3.1) in Proposition 3.1 (existence of the local-in-time solution) will be automatically deduced.

REMARK 4.2. Assumption (4.4) is related to the smallness assumption for the initial data $(\boldsymbol{\alpha}_0, \boldsymbol{a}_0)$. Namely, if the initial misorientations are sufficiently small and the position of the initial triple junction is sufficiently close to the position of the equilibrium triple junction $\boldsymbol{a}_\infty$, then we obtain (4.4).

Now we are in position to show the global existence of the solution of (2.3).

THEOREM 4.1 (Global existence). *Let* $\boldsymbol{x}^{(1)}, \boldsymbol{x}^{(2)}, \boldsymbol{x}^{(3)} \in \mathbb{R}^2$*,* $\boldsymbol{a}_0 \in \mathbb{R}^2$*, and* $\boldsymbol{\alpha}_0 \in \mathbb{R}^3$ *be the initial data for the system* (2.3)*. Assume* (2.8)*, and let* $\boldsymbol{a}_\infty$ *be a unique solution of the equilibrium system* (2.9)*. Further, assume condition* (4.4)*. Then there exists a unique global-in-time solution* $(\boldsymbol{\alpha}, \boldsymbol{a})$ *of* (2.3)*.*

Proof. We need to show that the solution given by Proposition 3.1 extends globally in time. Let $(\boldsymbol{\alpha}, \boldsymbol{a})$ be a solution of (2.3) on $0 \le t \le T$. By Lemma 4.1, we obtain $|\boldsymbol{a}(T) - \boldsymbol{a}_\infty| < \frac{1}{2}|\boldsymbol{b}_\infty^{(j)}|$. Due to Proposition 3.2 (energy dissipation), we also have,

$$E(T) = \sum_{j=1}^{3} \sigma(\Delta^{(j)}\alpha(T))|\boldsymbol{a}(T) - \boldsymbol{x}^{(j)}| \le E(0) < \sigma(0)C_1.$$

In addition, from Proposition 3.3 (maximum principle), we have that $|\boldsymbol{\alpha}(T)| \le |\boldsymbol{\alpha}_0|$, hence we can extend the solution globally in time. □

In the above proof, a key argument is how to obtain the a priori estimate for the position of the triple junction $\boldsymbol{a}$, Lemma 4.1. An energy smallness condition (4.4) plays an important role to obtain the a priori estimate for the solution of (2.3).

5. Large-time asymptotic behavior

In this section, large-time behavior of the global solution given by Theorem 4.1 is presented. We first discuss in Proposition 5.1 below large-time asymptotic profile of the solution of (2.3). After that, we show in Theorem 5.1 that the asymptotic profile is asymptotically exponentially stable.

PROPOSITION 5.1.   *Let* $\boldsymbol{x}^{(1)}$, $\boldsymbol{x}^{(2)}$, $\boldsymbol{x}^{(3)} \in \mathbb{R}^2$, $\boldsymbol{a}_0 \in \mathbb{R}^2$, *and* $\boldsymbol{\alpha}_0 \in \mathbb{R}^3$ *be the initial data for the system* (2.3). *We assume that the initial data satisfy* (4.4), *and we also impose the same assumptions as in Theorem* 4.1. *Define* α_∞ *as,*

$$\alpha_\infty := \frac{\alpha_0^{(1)} + \alpha_0^{(2)} + \alpha_0^{(3)}}{3}. \tag{5.1}$$

Let $\boldsymbol{a}_\infty$ *be a solution of the equilibrium system* (2.9) *and* $(\boldsymbol{\alpha}, \boldsymbol{a})$ *be a time-global solution of* (2.3). *Then,*

$$\boldsymbol{\alpha}(t) \to \alpha_\infty(1,1,1), \quad \boldsymbol{a}(t) \to \boldsymbol{a}_\infty, \tag{5.2}$$

as $t \to \infty$.

Proof.   Consider arbitrary time sequence $t_k \to \infty$. From Proposition 3.3 (maximum principle), Lemma 4.1 (boundedness of the triple junction), and Proposition 3.2 (energy dissipation), we have a convergent subsequence (denoted by the same $t_k \to \infty$) such that,

$$\begin{aligned} \boldsymbol{\alpha}(t_k) &\to \boldsymbol{\alpha}_{\infty,*}, & \boldsymbol{a}(t_k) &\to \boldsymbol{a}_{\infty,*}, \\ \left| \frac{d\boldsymbol{\alpha}}{dt}(t_k) \right| &\to 0, & \left| \frac{d\boldsymbol{a}}{dt}(t_k) \right| &\to 0, \end{aligned} \tag{5.3}$$

and,

$$|\boldsymbol{a}_{\infty,*} - \boldsymbol{a}_\infty| \leq \frac{1}{2}|\boldsymbol{a}_\infty - \boldsymbol{x}^{(j)}|, \tag{5.4}$$

for some $\boldsymbol{\alpha}_{\infty,*} \in \mathbb{R}^3$ and $\boldsymbol{a}_{\infty,*} \in \mathbb{R}^2$. We have to show $\boldsymbol{\alpha}_{\infty,*} = \alpha_\infty(1,1,1)$ and $\boldsymbol{a}_{\infty,*} = \boldsymbol{a}_\infty$. Taking the same limit with respect to t_k in the equation (2.3), from (5.3) we obtain,

$$\begin{cases} 0 = -\left(\sigma_\theta(\Delta^{(j+1)}\boldsymbol{\alpha}_{\infty,*})|\boldsymbol{b}_{\infty,*}^{(j+1)}| - \sigma_\theta(\Delta^{(j)}\boldsymbol{\alpha}_{\infty,*})|\boldsymbol{b}_{\infty,*}^{(j)}| \right), \\ \boldsymbol{0} = \sum_{j=1}^{3} \sigma(\Delta^{(j)}\boldsymbol{\alpha}_{\infty,*}) \frac{\boldsymbol{b}_{\infty,*}^{(j)}}{|\boldsymbol{b}_{\infty,*}^{(j)}|}, \\ \boldsymbol{a}_{\infty,*} = \boldsymbol{x}^{(1)} - \boldsymbol{b}_{\infty,*}^{(1)} = \boldsymbol{x}^{(2)} - \boldsymbol{b}_{\infty,*}^{(2)} = \boldsymbol{x}^{(3)} - \boldsymbol{b}_{\infty,*}^{(3)}. \end{cases} \tag{5.5}$$

We will show that $\Delta^{(j)}\boldsymbol{\alpha}_{\infty,*} = 0$ for $j = 1,2,3$. First, by (5.4), we have that,

$$|\boldsymbol{b}_{\infty,*}^{(j)}| = |\boldsymbol{x}^{(j)} - \boldsymbol{a}_{\infty,*}| \geq |\boldsymbol{x}^{(j)} - \boldsymbol{a}_\infty| - |\boldsymbol{a}_\infty - \boldsymbol{a}_{\infty,*}| \geq \frac{1}{2}|\boldsymbol{x}^{(j)} - \boldsymbol{a}_\infty| > 0.$$

Next, from the first equation of (5.5), we obtain

$$\sigma_\theta(\Delta^{(1)}\boldsymbol{\alpha}_{\infty,*})|\boldsymbol{b}_{\infty,*}^{(1)}| = \sigma_\theta(\Delta^{(2)}\boldsymbol{\alpha}_{\infty,*})|\boldsymbol{b}_{\infty,*}^{(2)}| = \sigma_\theta(\Delta^{(3)}\boldsymbol{\alpha}_{\infty,*})|\boldsymbol{b}_{\infty,*}^{(3)}|. \tag{5.6}$$

Multiplying (5.6) by $\Delta^{(2)}\boldsymbol{\alpha}_{\infty,*}$ and $\Delta^{(3)}\boldsymbol{\alpha}_{\infty,*}$, and using the convexity assumption (2.5), we have

$$\sigma_\theta(\Delta^{(1)}\boldsymbol{\alpha}_{\infty,*})(\Delta^{(2)}\boldsymbol{\alpha}_{\infty,*})|\boldsymbol{b}_{\infty,*}^{(1)}| \geq 0, \qquad \sigma_\theta(\Delta^{(1)}\boldsymbol{\alpha}_{\infty,*})(\Delta^{(3)}\boldsymbol{\alpha}_{\infty,*})|\boldsymbol{b}_{\infty,*}^{(1)}| \geq 0.$$

Thus $\Delta^{(1)}\boldsymbol{\alpha}_{\infty,*} = 0$ follows from $-\sigma_\theta(\Delta^{(1)}\boldsymbol{\alpha}_{\infty,*})(\Delta^{(1)}\boldsymbol{\alpha}_{\infty,*})|\boldsymbol{b}_{\infty,*}^{(1)}| \geq 0$ (obtained from the above), the assumptions (2.5) and (2.6). We can obtain $\Delta^{(2)}\boldsymbol{\alpha}_{\infty,*} = \Delta^{(3)}\boldsymbol{\alpha}_{\infty,*} = 0$ in a similar way.

From Lemma 3.1, (5.1), and $\Delta^{(j)}\alpha_{\infty,*}=0$ for $j=1,2,3$, we find, $\alpha_{\infty,*}^{(j)}=\alpha_\infty$ for all $j=1,2,3$. Again using (5.5), we obtain that,

$$\mathbf{0}=\sum_{j=1}^{3}\frac{\boldsymbol{b}_{\infty,*}^{(j)}}{|\boldsymbol{b}_{\infty,*}^{(j)}|}.$$

Therefore, by uniqueness of the Fermat-Torricelli problem, we obtain $\boldsymbol{a}_{\infty,*}=\boldsymbol{a}_\infty$ (cf. the Fermat-Torricelli Problem [7, Theorem 18.3]). □

Hereafter we denote $\boldsymbol{\alpha}_\infty:=\alpha_\infty(1,1,1)$. To prove the exponential stability for $(\boldsymbol{\alpha}_\infty,\boldsymbol{a}_\infty)$ of the system (2.3), we study the linearized problem of (2.3) and show the decay properties of the solution to the linearized problem, Propositions 5.2 and 5.3. We first derive the linearized problem in Lemma 5.1.

LEMMA 5.1 (Linearized problem). *The linearized problem of* (2.3) *around* $(\boldsymbol{\alpha}_\infty,\boldsymbol{a}_\infty)$ *is given as,*

$$\begin{cases}\dfrac{d\boldsymbol{\alpha}_L}{dt}=-\gamma\sigma_{\theta\theta}(0)\mathbb{B}_\infty\boldsymbol{\alpha}_L,\quad \mathbb{B}_\infty=\begin{pmatrix}|\boldsymbol{b}_\infty^{(1)}|+|\boldsymbol{b}_\infty^{(2)}| & -|\boldsymbol{b}_\infty^{(2)}| & -|\boldsymbol{b}_\infty^{(1)}| \\ -|\boldsymbol{b}_\infty^{(2)}| & |\boldsymbol{b}_\infty^{(2)}|+|\boldsymbol{b}_\infty^{(3)}| & -|\boldsymbol{b}_\infty^{(3)}| \\ -|\boldsymbol{b}_\infty^{(1)}| & -|\boldsymbol{b}_\infty^{(3)}| & |\boldsymbol{b}_\infty^{(3)}|+|\boldsymbol{b}_\infty^{(1)}|\end{pmatrix}, \\[4mm] \dfrac{d\boldsymbol{a}_L}{dt}=-\eta\sigma(0)\sum_{j=1}^{3}\left(\dfrac{1}{|\boldsymbol{b}_\infty^{(j)}|}\left(I-\dfrac{\boldsymbol{b}_\infty^{(j)}}{|\boldsymbol{b}_\infty^{(j)}|}\otimes\dfrac{\boldsymbol{b}_\infty^{(j)}}{|\boldsymbol{b}_\infty^{(j)}|}\right)\right)\boldsymbol{a}_L=:-\eta\sigma(0)L_{\boldsymbol{a}}\boldsymbol{a}_L, \\[4mm] \sum_{j=1}^{3}\dfrac{\boldsymbol{b}_\infty^{(j)}}{|\boldsymbol{b}_\infty^{(j)}|}=\mathbf{0},\end{cases} \tag{5.7}$$

where $\otimes$ *denotes the outer product of two vectors.*

Proof. In order to obtain the linearized problem (5.7), we consider,

$$\boldsymbol{\alpha}(t)=\boldsymbol{\alpha}_\infty+\varepsilon\boldsymbol{\alpha}_L(t),\quad \boldsymbol{a}(t)=\boldsymbol{a}_\infty+\varepsilon\boldsymbol{a}_L(t), \tag{5.8}$$

in (2.3), and take a derivative with respect to ε. Note, the third equation in (5.7) came from the equilibrium system (2.9), so we will only derive the equations for $\boldsymbol{\alpha}_L$ and $\boldsymbol{a}_L$. First, we derive the equation for $\boldsymbol{\alpha}_L$ (the first equation in (5.7)). Since $\Delta^{(j)}\alpha=\varepsilon\Delta^{(j)}\alpha_L$ and $\sigma_\theta(0)=0$, we compute,

$$\frac{d}{d\varepsilon}\Big|_{\varepsilon=0}\left(-\Big(\sigma_\theta(\Delta^{(j+1)}\alpha)|\boldsymbol{b}^{(j+1)}|-\sigma_\theta(\Delta^{(j)}\alpha)|\boldsymbol{b}^{(j)}|\Big)\right)$$

$$=\frac{d}{d\varepsilon}\Big|_{\varepsilon=0}\left(-\Big(\sigma_\theta(\varepsilon\Delta^{(j+1)}\alpha_L)|\boldsymbol{x}^{(j+1)}-\boldsymbol{a}_\infty-\varepsilon\boldsymbol{a}_L|-\sigma_\theta(\varepsilon\Delta^{(j)}\alpha_L)|\boldsymbol{x}^{(j)}-\boldsymbol{a}_\infty-\varepsilon\boldsymbol{a}_L|\Big)\right)$$

$$=-\sigma_{\theta\theta}(\varepsilon\Delta^{(j+1)}\alpha_L)\Delta^{(j+1)}\alpha_L|\boldsymbol{x}^{(j+1)}-\boldsymbol{a}_\infty-\varepsilon\boldsymbol{a}_L|$$

$$\quad+\sigma_\theta(\varepsilon\Delta^{(j+1)}\alpha_L)\frac{(\boldsymbol{x}^{(j+1)}-\boldsymbol{a}_\infty-\varepsilon\boldsymbol{a}_L)\cdot\boldsymbol{a}_L}{|\boldsymbol{x}^{(j+1)}-\boldsymbol{a}_\infty-\varepsilon\boldsymbol{a}_L|}$$

$$\quad+\sigma_{\theta\theta}(\varepsilon\Delta^{(j)}\alpha_L)\Delta^{(j)}\alpha_L|\boldsymbol{x}^{(j)}-\boldsymbol{a}_\infty-\varepsilon\boldsymbol{a}_L|-\sigma_\theta(\varepsilon\Delta^{(j)}\alpha_L)\frac{(\boldsymbol{x}^{(j)}-\boldsymbol{a}_\infty-\varepsilon\boldsymbol{a}_L)\cdot\boldsymbol{a}_L}{|\boldsymbol{x}^{(j)}-\boldsymbol{a}_\infty-\varepsilon\boldsymbol{a}_L|}\Big|_{\varepsilon=0}$$

$$=-\sigma_{\theta\theta}(0)\Delta^{(j+1)}\alpha_L|\boldsymbol{b}_\infty^{(j+1)}|+\sigma_{\theta\theta}(0)\Delta^{(j)}\alpha_L|\boldsymbol{b}_\infty^{(j)}|$$

$$=-\sigma_{\theta\theta}(0)\left((|\boldsymbol{b}_\infty^{(j+1)}|+|\boldsymbol{b}_\infty^{(j)}|)\alpha_L^{(j)}-|\boldsymbol{b}_\infty^{(j+1)}|\alpha_L^{(j+1)}-|\boldsymbol{b}_\infty^{(j)}|\alpha_L^{(j-1)}\right).$$

Next, we will elaborate on some details of the right-hand side of the equation for $\boldsymbol{a}_L$ (the second equation in (5.7)). Since $\sigma_\theta(0) = 0$, we compute,

$$\frac{d}{d\varepsilon}\bigg|_{\varepsilon=0}\left(\sigma(\Delta^{(j)}\alpha)\frac{\boldsymbol{b}^{(j)}}{|\boldsymbol{b}^{(j)}|}\right)$$

$$=\frac{d}{d\varepsilon}\bigg|_{\varepsilon=0}\left(\sum_{j=1}^3 \sigma(\varepsilon\Delta^{(j)}\alpha_L)\frac{\boldsymbol{x}^{(j)}-\boldsymbol{a}_\infty-\varepsilon\boldsymbol{a}_L}{|\boldsymbol{x}^{(j)}-\boldsymbol{a}_\infty-\varepsilon\boldsymbol{a}_L|}\right)$$

$$=\left(\sum_{j=1}^3 \sigma_\theta(\varepsilon\Delta^{(j)}\alpha_L)\Delta^{(j)}\alpha_L\frac{\boldsymbol{x}^{(j)}-\boldsymbol{a}_\infty-\varepsilon\boldsymbol{a}_L}{|\boldsymbol{x}^{(j)}-\boldsymbol{a}_\infty-\varepsilon\boldsymbol{a}_L|}\right.$$

$$\left.+\sigma(\varepsilon\Delta^{(j)}\alpha_L)\left(\frac{-\boldsymbol{a}_L}{|\boldsymbol{x}^{(j)}-\boldsymbol{a}_\infty-\varepsilon\boldsymbol{a}_L|}+\frac{(\boldsymbol{x}^{(j)}-\boldsymbol{a}_\infty-\varepsilon\boldsymbol{a}_L)\cdot\boldsymbol{a}_L}{|\boldsymbol{x}^{(j)}-\boldsymbol{a}_\infty-\varepsilon\boldsymbol{a}_L|^3}(\boldsymbol{x}^{(j)}-\boldsymbol{a}_\infty-\varepsilon\boldsymbol{a}_L)\right)\right)\bigg|_{\varepsilon=0}$$

$$=\sigma(0)\sum_{j=1}^3\left(\frac{-\boldsymbol{a}_L}{|\boldsymbol{b}_\infty^{(j)}|}+\frac{(\boldsymbol{b}_\infty^{(j)}\cdot\boldsymbol{a}_L)}{|\boldsymbol{b}_\infty^{(j)}|^3}\boldsymbol{b}_\infty^{(j)}\right)=-\sigma(0)\sum_{j=1}^3\frac{1}{|\boldsymbol{b}_\infty^{(j)}|}\left(\boldsymbol{a}_L-\frac{(\boldsymbol{b}_\infty^{(j)}\cdot\boldsymbol{a}_L)}{|\boldsymbol{b}_\infty^{(j)}|^2}\boldsymbol{b}_\infty^{(j)}\right).$$

Note, that the term,

$$\frac{(\boldsymbol{b}_\infty^{(j)}\cdot\boldsymbol{a}_L)}{|\boldsymbol{b}_\infty^{(j)}|^2}\boldsymbol{b}_\infty^{(j)}=\left(\frac{\boldsymbol{b}_\infty^{(j)}}{|\boldsymbol{b}_\infty^{(j)}|}\cdot\boldsymbol{a}_L\right)\frac{\boldsymbol{b}_\infty^{(j)}}{|\boldsymbol{b}_\infty^{(j)}|}=\left(\frac{\boldsymbol{b}_\infty^{(j)}}{|\boldsymbol{b}_\infty^{(j)}|}\otimes\frac{\boldsymbol{b}_\infty^{(j)}}{|\boldsymbol{b}_\infty^{(j)}|}\right)\boldsymbol{a}_L,$$

where $\otimes$ denotes the outer product of two vectors. □

It is important to note that, in the linearized problem (5.7), we consider a matrix of the form, for c_1, c_2, $c_3 \in \mathbb{R}$,

$$\mathbb{C}:=\begin{pmatrix} c_1+c_2 & -c_2 & -c_1 \\ -c_2 & c_2+c_3 & -c_3 \\ -c_1 & -c_3 & c_3+c_1 \end{pmatrix}. \tag{5.9}$$

By direct calculation, it can be shown that the eigenvalues of such matrix $\mathbb{C}$ (5.9) are

$$0 \text{ and } c_1+c_2+c_3\pm\sqrt{\frac{1}{2}\left((c_1-c_2)^2+(c_2-c_3)^2+(c_3-c_1)^2\right)}.$$

If c_1, c_2, $c_3 \geq 0$, then the matrix $\mathbb{C}$ is non-negative definite. Furthermore, if c_1, c_2, $c_3 > 0$, then the zero eigenvalue of $\mathbb{C}$ is simple, and $(1,1,1)$ is an eigenvector associated with the zero eigenvalue.

Next proposition gives the decay properties for solutions $\boldsymbol{\alpha}_L$ of (5.7).

PROPOSITION 5.2.   *Let $\boldsymbol{\alpha}_L$ be a solution of (5.7). Assume that, $\boldsymbol{\alpha}_L(0)\cdot(1,1,1)=0$. Then, there exists a positive constant $\lambda_1 > 0$ which depends only on $|\boldsymbol{b}_\infty^{(j)}|$, such that,*

$$|\boldsymbol{\alpha}_L(t)|\leq e^{-\gamma\sigma_{\theta\theta}(0)\lambda_1 t}|\boldsymbol{\alpha}_L(0)|. \tag{5.10}$$

Proof.   Using (5.7) and $\mathbb{B}_\infty(1,1,1)=\boldsymbol{0}$, we have that,

$$\frac{d}{dt}(\boldsymbol{\alpha}_L\cdot(1,1,1))=-\gamma\sigma_{\theta\theta}(0)\mathbb{B}_\infty\boldsymbol{\alpha}_L\cdot(1,1,1)=-\gamma\sigma_{\theta\theta}(0)\boldsymbol{\alpha}_L\cdot\mathbb{B}_\infty(1,1,1)=0,$$

hence, $\boldsymbol{\alpha}_L\cdot(1,1,1)=\boldsymbol{\alpha}_L(0)\cdot(1,1,1)=0$. Define,

$$\lambda_1:=|\boldsymbol{b}_\infty^{(1)}|+|\boldsymbol{b}_\infty^{(2)}|+|\boldsymbol{b}_\infty^{(3)}|-\sqrt{\frac{1}{2}\left((|\boldsymbol{b}_\infty^{(1)}|-|\boldsymbol{b}_\infty^{(2)}|)^2+(|\boldsymbol{b}_\infty^{(2)}|-|\boldsymbol{b}_\infty^{(3)}|)^2+(|\boldsymbol{b}_\infty^{(3)}|-|\boldsymbol{b}_\infty^{(1)}|)^2\right)}, \tag{5.11}$$

which is the smallest positive eigenvalue of $\mathbb{B}_\infty$. Since $|\boldsymbol{b}_\infty^{(j)}| > 0$ for all $j = 1, 2, 3$, and $\boldsymbol{\alpha}_L \cdot (1, 1, 1) = 0$, we find that $\boldsymbol{\alpha}_L$ is a linear combination of the eigenvectors associated with the positive eigenvalues of $\mathbb{B}_\infty$. Thus, we obtain,

$$\frac{d}{dt}|\boldsymbol{\alpha}_L(t)|^2 = -2\gamma\sigma_{\theta\theta}(0)\mathbb{B}_\infty\boldsymbol{\alpha}_L(t) \cdot \boldsymbol{\alpha}_L(t) \leq -2\gamma\sigma_{\theta\theta}(0)\lambda_1|\boldsymbol{\alpha}_L(t)|^2.$$

By the Gronwall's inequality, we obtain (5.10). □

In order to derive decay properties for the solution $\boldsymbol{a}_L$ of (5.7) in Proposition 5.2, we first show below that $L_{\boldsymbol{a}}$ is positive definite.

LEMMA 5.2. *There exists a positive constant $\lambda_2 > 0$, which depends only on $\boldsymbol{b}_\infty^{(j)}$, such that,*

$$L_{\boldsymbol{a}} := \sum_{j=1}^{3} \frac{1}{|\boldsymbol{b}_\infty^{(j)}|} \left(I - \frac{\boldsymbol{b}_\infty^{(j)}}{|\boldsymbol{b}_\infty^{(j)}|} \otimes \frac{\boldsymbol{b}_\infty^{(j)}}{|\boldsymbol{b}_\infty^{(j)}|} \right) \geq \lambda_2 I. \tag{5.12}$$

Proof. For $\boldsymbol{\xi} \in \mathbb{R}^2$, we have that,

$$\left(\sum_{j=1}^{3} \frac{1}{|\boldsymbol{b}_\infty^{(j)}|} \left(I - \frac{\boldsymbol{b}_\infty^{(j)}}{|\boldsymbol{b}_\infty^{(j)}|} \otimes \frac{\boldsymbol{b}_\infty^{(j)}}{|\boldsymbol{b}_\infty^{(j)}|} \right) \boldsymbol{\xi} \cdot \boldsymbol{\xi} \right) = \sum_{j=1}^{3} \frac{1}{|\boldsymbol{b}_\infty^{(j)}|} \left(|\boldsymbol{\xi}|^2 - \left(\frac{\boldsymbol{b}_\infty^{(j)}}{|\boldsymbol{b}_\infty^{(j)}|} \cdot \boldsymbol{\xi} \right)^2 \right) \geq 0,$$

hence, we obtain (5.12) with some non-negative constant $\lambda_2 \geq 0$.

Assume now that $\lambda_2 = 0$, then there is $\boldsymbol{\xi}_0 \in \mathbb{S}^1$ such that,

$$\sum_{j=1}^{3} \frac{1}{|\boldsymbol{b}_\infty^{(j)}|} \left(1 - \left(\frac{\boldsymbol{b}_\infty^{(j)}}{|\boldsymbol{b}_\infty^{(j)}|} \cdot \boldsymbol{\xi}_0 \right)^2 \right) = 0.$$

Thus, $\boldsymbol{\xi}_0$ has to be parallel to all $\boldsymbol{b}_\infty^{(j)}$ for $j = 1, 2, 3$. This is a contradiction to the dimension of $\mathbb{R}^2$. □

The convergence rate of the global solution to the equilibrium state depends on the decay rate of the linearized solution, hence it is important to give estimates for the constant λ_2. We will give an explicit form of λ_2 in the Appendix. As a matter of fact from detailed calculations in the Appendix, the constant λ_2 depends only on $|\boldsymbol{b}_\infty^{(j)}|$, see (7.5).

Similar to the result of Proposition 5.2, we have,

PROPOSITION 5.3. *Let $\boldsymbol{a}_L(t)$ be a solution of (5.7). Then,*

$$|\boldsymbol{a}_L(t)| \leq e^{-\eta\sigma(0)\lambda_2 t}|\boldsymbol{a}_L(0)|, \tag{5.13}$$

for all $t > 0$, and the constant $\lambda_2 > 0$ is given by Lemma 5.2.

Denote,

$$\lambda := \min\{\gamma\sigma_{\theta\theta}(0)\lambda_1, \eta\sigma(0)\lambda_2\}, \tag{5.14}$$

where λ_1, λ_2 are given in Propositions 5.2, and 5.3, respectively.

REMARK 5.1. Note that λ_1, λ_2 are derived from eigenvalues of the linearized problem (5.7). The constant λ_1 is the smallest positive eigenvalue of the linearized operator for

the equation of the orientations $\boldsymbol{\alpha}$, see Proposition 5.2 and (5.11). The constant λ_2 is the smallest eigenvalue of the linearized operator for the equation of the triple junction $\boldsymbol{a}$, see Lemma 5.2, Proposition 5.3, and (7.5).

For a solution $(\boldsymbol{\alpha}, \boldsymbol{a})$ of (2.3), define $\boldsymbol{\alpha}_p$ and $\boldsymbol{a}_p$ as,

$$\boldsymbol{\alpha} = \boldsymbol{\alpha}_\infty + \boldsymbol{\alpha}_p, \quad \boldsymbol{a} = \boldsymbol{a}_\infty + \boldsymbol{a}_p. \tag{5.15}$$

Then $\boldsymbol{\alpha}_p$ and $\boldsymbol{a}_p$ satisfy,

$$\begin{cases} (\boldsymbol{\alpha}_p)_t = -\gamma \sigma_{\theta\theta}(0)\mathbb{B}_\infty \boldsymbol{\alpha}_p + \gamma\left(\sigma_{\theta\theta}(0)\mathbb{B}_\infty \boldsymbol{\alpha}_p - \boldsymbol{\Phi}(\boldsymbol{\alpha}, \boldsymbol{a})\right), \\ (\boldsymbol{a}_p)_t = -\eta\sigma(0)L_{\boldsymbol{a}}\boldsymbol{a}_p + \eta\sum_{j=1}^{3}\left(\frac{\sigma(0)}{|\boldsymbol{b}_\infty^{(j)}|}\left(I - \frac{\boldsymbol{b}_\infty^{(j)}}{|\boldsymbol{b}_\infty^{(j)}|}\otimes\frac{\boldsymbol{b}_\infty^{(j)}}{|\boldsymbol{b}_\infty^{(j)}|}\right)\boldsymbol{a}_p + \sigma(\Delta^{(j)}\alpha)\frac{\boldsymbol{b}^{(j)}}{|\boldsymbol{b}^{(j)}|}\right), \\ \boldsymbol{\alpha}_p(0) = \boldsymbol{\alpha}_0 - \boldsymbol{\alpha}_\infty, \quad \boldsymbol{a}_p(0) = \boldsymbol{a}_0 - \boldsymbol{a}_\infty, \end{cases} \tag{5.16}$$

where $L_{\boldsymbol{a}}$ is defined as in (5.12) and $\boldsymbol{\Phi}(\boldsymbol{\alpha}, \boldsymbol{a})$ is given by

$$\boldsymbol{\Phi}(\boldsymbol{\alpha}, \boldsymbol{a}) = \left(\Phi^{(j)}(\boldsymbol{\alpha}, \boldsymbol{a})\right)_j, \quad \Phi^{(j)}(\boldsymbol{\alpha}, \boldsymbol{a}) = \sigma_\theta(\Delta^{(j+1)}\alpha)|\boldsymbol{b}^{(j+1)}| - \sigma_\theta(\Delta^{(j)}\alpha)|\boldsymbol{b}^{(j)}|.$$

Note that the first equation of the original problem (2.3) can be written as $\boldsymbol{\alpha}_t = -\gamma\boldsymbol{\Phi}(\boldsymbol{\alpha}, \boldsymbol{a})$.

In the next two Lemmas 5.3 and 5.4, we will show the decay estimates for the perturbation terms $\boldsymbol{\alpha}_p$, $\boldsymbol{a}_p$.

LEMMA 5.3.   *Let $(\boldsymbol{\alpha}, \boldsymbol{a})$ be a global solution of (2.3), and let $\boldsymbol{\alpha}_p$ and $\boldsymbol{a}_p$ be defined as in (5.15). Then, there are positive constants $C_2 > 0$ and $\varepsilon_1 > 0$, such that, if $|\boldsymbol{\alpha}_p(t)| + |\boldsymbol{a}_p(t)| < \varepsilon_1$ for all $t > 0$, then*

$$e^{\lambda t}|\boldsymbol{\alpha}_p(t)| \le |\boldsymbol{\alpha}_p(0)| + C_2\int_0^t e^{\lambda s}(|\boldsymbol{\alpha}_p(s)|^2 + |\boldsymbol{a}_p(s)|^2)\,ds. \tag{5.17}$$

Proof.   By the Duhamel principle,

$$\boldsymbol{\alpha}_p(t) = e^{-t\gamma\sigma_{\theta\theta}(0)\mathbb{B}_\infty}\boldsymbol{\alpha}_p(0) + \gamma\int_0^t e^{-(t-s)\gamma\sigma_{\theta\theta}(0)\mathbb{B}_\infty}\left(\sigma_{\theta\theta}(0)\mathbb{B}_\infty\boldsymbol{\alpha}_p(s) - \boldsymbol{\Phi}(\boldsymbol{\alpha}(s), \boldsymbol{a}(s))\right)ds. \tag{5.18}$$

Since $\boldsymbol{\alpha}_0\cdot(1,1,1) = \boldsymbol{\alpha}_\infty\cdot(1,1,1)$, $\boldsymbol{\alpha}_p(0)$ is perpendicular to the vector $(1,1,1)$. Also the function $\sigma_{\theta\theta}(0)\mathbb{B}_\infty\boldsymbol{\alpha}_p(s) - \boldsymbol{\Phi}(\boldsymbol{\alpha}(s), \boldsymbol{a}(s))$ is also perpendicular to the vector $(1,1,1)$ for all $s > 0$, since $\mathbb{B}_\infty\boldsymbol{\alpha}_p\cdot(1,1,1) = \boldsymbol{\Phi}\cdot(1,1,1) = 0$. By Proposition 5.2 we obtain that,

$$|e^{-t\gamma\sigma_{\theta\theta}(0)\mathbb{B}_\infty}\boldsymbol{\alpha}_p(0)| \le e^{-\lambda t}|\boldsymbol{\alpha}_p(0)|, \tag{5.19}$$

and

$$\left|e^{-(t-s)\gamma\sigma_{\theta\theta}(0)\mathbb{B}_\infty}\left(\sigma_{\theta\theta}(0)\mathbb{B}_\infty\boldsymbol{\alpha}_p(s) - \boldsymbol{\Phi}(\boldsymbol{\alpha}(s), \boldsymbol{a}(s))\right)\right|$$
$$\le e^{-\lambda(t-s)}|\sigma_{\theta\theta}(0)\mathbb{B}_\infty\boldsymbol{\alpha}_p(s) - \boldsymbol{\Phi}(\boldsymbol{\alpha}(s), \boldsymbol{a}(s))|. \tag{5.20}$$

By the Taylor expansion $\boldsymbol{\Phi}(\boldsymbol{\alpha}, \boldsymbol{a})$ around $(\boldsymbol{\alpha}_\infty, \boldsymbol{a}_\infty)$, we obtain

$$\boldsymbol{\Phi}(\boldsymbol{\alpha}, \boldsymbol{a}) = \sigma_{\theta\theta}(0)\mathbb{B}_\infty\boldsymbol{\alpha}_p + O\left(|\boldsymbol{\alpha}_p|^2 + |\boldsymbol{a}_p|^2\right), \quad \text{as } |\boldsymbol{\alpha}_p| + |\boldsymbol{a}_p| \to 0.$$

Hence, there are $C_2 > 0$ and $\varepsilon_1 > 0$ such that, if $|\boldsymbol{\alpha}_p| + |\boldsymbol{a}_p| < \varepsilon_1$,

$$|\sigma_{\theta\theta}(0)\mathbb{B}_\infty \boldsymbol{\alpha}_p(s) - \boldsymbol{\Phi}(\boldsymbol{\alpha}(s), \boldsymbol{a}(s))| \leq C_2(|\boldsymbol{\alpha}_p|^2 + |\boldsymbol{a}_p|^2). \tag{5.21}$$

Using the estimates (5.19), (5.20) and (5.21) in (5.18), we obtain the result (5.17). □

LEMMA 5.4.   *Let $(\boldsymbol{\alpha}, \boldsymbol{a})$ be a global solution of (2.3), and let $\boldsymbol{\alpha}_p$ and $\boldsymbol{a}_p$ be defined as in (5.15). Then, there are positive constants $C_3 > 0$ and $\varepsilon_2 > 0$, such that, if $|\boldsymbol{\alpha}_p(t)| + |\boldsymbol{a}_p(t)| < \varepsilon_2$ for all $t > 0$, then,*

$$e^{\lambda t}|\boldsymbol{a}_p(t)| \leq |\boldsymbol{a}_p(0)| + C_3 \int_0^t e^{\lambda s} \left(|\boldsymbol{\alpha}_p(s)|^2 + |\boldsymbol{a}_p(s)|^2 \right) ds, \tag{5.22}$$

for all $t > 0$.

Proof.   By the Duhamel principle for (5.16), we have,

$$\boldsymbol{a}_p(t) = e^{-t\eta\sigma(0)L_{\boldsymbol{a}}} \boldsymbol{a}_p(0) + \eta \int_0^t e^{-(t-s)\eta\sigma(0)L_{\boldsymbol{a}}} F(s) \, ds, \tag{5.23}$$

where

$$F(s) := \sum_{j=1}^3 \left(\frac{\sigma(0)}{|\boldsymbol{b}_\infty^{(j)}|} \left(I - \frac{\boldsymbol{b}_\infty^{(j)}}{|\boldsymbol{b}_\infty^{(j)}|} \otimes \frac{\boldsymbol{b}_\infty^{(j)}}{|\boldsymbol{b}_\infty^{(j)}|} \right) \boldsymbol{a}_p + \sigma(\Delta^{(j)}\alpha) \frac{\boldsymbol{b}^{(j)}}{|\boldsymbol{b}^{(j)}|} \right). \tag{5.24}$$

By Lemma 5.2 and Proposition 5.3, we obtain,

$$|\boldsymbol{a}_p(t)| \leq e^{-\lambda t}|\boldsymbol{\alpha}_p(0)| + \eta \int_0^t e^{-\lambda(t-s)} |F(s)| \, ds. \tag{5.25}$$

Next, by the Taylor expansion of $\sigma(\Delta^{(j)}\alpha)\boldsymbol{b}^{(j)}/|\boldsymbol{b}^{(j)}|$ around $(\boldsymbol{\alpha}_\infty, \boldsymbol{a}_\infty)$, we obtain,

$$\sum_{j=1}^3 \sigma(\Delta^{(j)}\alpha) \frac{\boldsymbol{b}^{(j)}}{|\boldsymbol{b}^{(j)}|} = -\sum_{j=1}^3 \frac{\sigma(0)}{|\boldsymbol{b}_\infty^{(j)}|} \left(I - \frac{\boldsymbol{b}_\infty^{(j)}}{|\boldsymbol{b}_\infty^{(j)}|} \otimes \frac{\boldsymbol{b}_\infty^{(j)}}{|\boldsymbol{b}_\infty^{(j)}|} \right) \boldsymbol{a}_p + O(|\boldsymbol{\alpha}_p|^2 + |\boldsymbol{a}_p|^2),$$

$$\text{as } |\boldsymbol{\alpha}_p| + |\boldsymbol{a}_p| \to 0. \tag{5.26}$$

Using, (5.26) in (5.24), we obtain,

$$F(s) = O(|\boldsymbol{\alpha}_p|^2 + |\boldsymbol{a}_p|^2), \quad \text{as } |\boldsymbol{\alpha}_p| + |\boldsymbol{a}_p| \to 0. \tag{5.27}$$

Hence, there are $C_3 > 0$ and $\varepsilon_2 > 0$ such that, if $|\boldsymbol{\alpha}_p| + |\boldsymbol{a}_p| < \varepsilon_2$,

$$|F(s)| \leq C_3 \left(|\boldsymbol{\alpha}_p|^2 + |\boldsymbol{a}_p|^2 \right). \tag{5.28}$$

Using estimate (5.28) in (5.25), we conclude with the desired estimate (5.22) on $\boldsymbol{a}_p(t)$.
□

Now we are in position to show exponential stability of the asymptotic profile of the solution of the system (2.3).

THEOREM 5.1.   *There is a small constant $\varepsilon_3 > 0$ such that, if $|\boldsymbol{\alpha}_0 - \boldsymbol{\alpha}_\infty| + |\boldsymbol{a}_0 - \boldsymbol{a}_\infty| < \varepsilon_3$, then the associated global solution $(\boldsymbol{\alpha}, \boldsymbol{a})$ of the system (2.3) satisfies,*

$$|\boldsymbol{\alpha}(t) - \boldsymbol{\alpha}_\infty| + |\boldsymbol{a}(t) - \boldsymbol{a}_\infty| \leq C_4 e^{-\lambda^* t}, \tag{5.29}$$

for some positive constants $C_4, \lambda^\star > 0$. The decay order $\lambda^\star$ is explicitly estimated as,

$$\lambda^\star \geq \lambda, \tag{5.30}$$

where λ is defined in (5.14).

Proof. Let $\boldsymbol{\alpha}_p$ and $\boldsymbol{a}_p$ be defined as in (5.15), and define $V(t) := e^{\lambda t} |\boldsymbol{\alpha}_p(t)|$ and $W(t) := e^{\lambda t} |\boldsymbol{a}_p(t)|$. Next, take sufficiently small $0 < \varepsilon_3 < \min\{\varepsilon_1, \varepsilon_2\}/2$ such that (4.4) is fulfilled if an initial data $(\boldsymbol{\alpha}_0, \boldsymbol{a}_0)$ satisfy $|\boldsymbol{\alpha}_0 - \boldsymbol{\alpha}_\infty| + |\boldsymbol{a}_0 - \boldsymbol{a}_\infty| < \varepsilon_3$. Here, the constants ε_1 and ε_2 are given in Lemmas 5.3 and 5.4, and assume that $|\boldsymbol{\alpha}_0 - \boldsymbol{\alpha}_\infty| + |\boldsymbol{a}_0 - \boldsymbol{a}_\infty| < \varepsilon_3$, namely $|\boldsymbol{\alpha}_p(0)| + |\boldsymbol{a}_p(0)| < \varepsilon_3$. In order to show (5.29), it is enough to show the boundedness for $V(t) + W(t)$. Now, assume $V(t) + W(t) < 2\varepsilon_3$ for $0 \leq t < t_0$ and $V(t_0) + W(t_0) = 2\varepsilon_3$. Note that, $V(t) + W(t) < \varepsilon_1, \varepsilon_2$ for $0 < t < t_0$, thus we can apply Lemmas 5.3 and 5.4. Therefore, from (5.17), (5.22) and that $V(t), W(t) \leq 2\varepsilon_3$ for $0 < t \leq t_0$, we obtain,

$$V(t) + W(t) \leq V(0) + W(0) + \frac{C_5}{2} \int_0^t e^{-\lambda s} (V^2(s) + W^2(s)) \, ds$$

$$\leq \varepsilon_3 + C_5 \varepsilon_3 \int_0^t e^{-\lambda s} (V(s) + W(s)) \, ds, \tag{5.31}$$

where $C_5 = 2(C_2 + C_3) > 0$. Applying the Gronwall's inequality to (5.31), we have that,

$$V(t) + W(t) \leq \varepsilon_3 + C_5 \varepsilon_3^2 \int_0^t e^{-\lambda s} \exp\left(C_5 \varepsilon_3 \int_s^t e^{-\lambda u} \, du \right) ds, \quad 0 \leq t \leq t_0. \tag{5.32}$$

Hence, we can easily obtain that,

$$C_5 \varepsilon_3^2 \int_0^t e^{-\lambda s} \exp\left(C_5 \varepsilon_3 \int_s^t e^{-\lambda u} \, du \right) ds \leq \frac{C_5 \varepsilon_3^2}{\lambda} \exp\left(\frac{C_5 \varepsilon_3}{\lambda} \right).$$

Thus, if we take $\varepsilon_3 > 0$ sufficiently small as,

$$\frac{C_5 \varepsilon_3}{\lambda} \exp\left(\frac{C_5 \varepsilon_3}{\lambda} \right) < 1, \tag{5.33}$$

then we deduce that $V(t_0) + W(t_0) < 2\varepsilon_3$, which contradicts the definition of t_0 above. Therefore, $V(t) + W(t)$ is bounded for $0 < t < \infty$, and we obtain (5.29). □

REMARK 5.2. Note that our argument is based on the uniqueness of the equilibrium state for the system (2.9). Otherwise, we can not recover full convergence in time as in Proposition 5.1. However, thanks to the uniqueness of the equilibrium state (2.9), we can consider the linearized problem (5.7) around the equilibrium state, and we can obtain the exponential uniform estimate (5.29) for the solution of the system (2.3).

Note also, that by Theorem 5.1, we obtain exponential decay of the total grain boundary energy to the equilibrium energy, that is

COROLLARY 5.1. *Under the same assumption as in Theorem 5.1, the associated grain boundary energy $E(t)$ satisfies,*

$$E(t) - E_\infty \leq C_6 e^{-\lambda^\star t}, \tag{5.34}$$

for some positive constant $C_6 > 0$, where

$$E_\infty := \sigma(0) \sum_{j=1}^{3} |\boldsymbol{b}_\infty^{(j)}|.$$

Proof. Since $\alpha_\infty^{(1)} = \alpha_\infty^{(2)} = \alpha_\infty^{(3)}$, we obtain

$$
\begin{aligned}
E(t) - E_\infty &= \sum_{j=1}^{3} \Big(\sigma(\Delta^{(j)}\alpha(t)) |\boldsymbol{b}^{(j)}(t)| - \sigma(0) |\boldsymbol{b}_\infty^{(j)}| \Big) \\
&\leq \sum_{j=1}^{3} \Big(\sigma(0) |\boldsymbol{b}^{(j)}(t) - \boldsymbol{b}_\infty^{(j)}| + \Big(\sigma(\Delta^{(j)}\alpha(t)) - \sigma(0) \Big) |\boldsymbol{b}^{(j)}(t)| \Big) \\
&\leq \sum_{j=1}^{3} \Big(\sigma(0) |\boldsymbol{a}^{(j)}(t) - \boldsymbol{a}_\infty| + \Big(C_7 |\Delta^{(j)}\alpha(t)| \Big) |\boldsymbol{b}^{(j)}(t)| \Big) \\
&\leq \sum_{j=1}^{3} \Big(\sigma(0) |\boldsymbol{a}^{(j)}(t) - \boldsymbol{a}_\infty| + 2C_7 |\boldsymbol{b}^{(j)}(t)| |\boldsymbol{\alpha}(t) - \boldsymbol{\alpha}_\infty| \Big),
\end{aligned}
\tag{5.35}
$$

where $C_7 = \sup_{|\theta| < 2\varepsilon_3} |\sigma_\theta(\theta)|$. Using the dissipation estimate (3.4) and the exponential decay estimate (5.29), we obtain (5.34). □

REMARK 5.3. Note, that the obtained exponential decay to equilibrium, see estimates (5.29) and (5.34), is obtained by considering linearized problem, Lemma 5.1. Consideration of the nonlinear problem instead could lead to potential power laws estimates for the decay rates. See also discussion and numerical experiments in Section 7.

6. Extension to grain boundary network

In this section, we extend our results to a grain boundary network $\{\Gamma_t^{(j)}\}_j$. As in, for example, [15], we define the total grain boundary energy of the network, like,

$$E(t) = \sum_{j} \sigma(\Delta^{(j)}\alpha) |\Gamma_t^{(j)}|, \tag{6.1}$$

where $\Delta^{(j)}\alpha$ is a misorientation, a difference between the lattice orientation of the two neighboring grains which form the grain boundary $\Gamma^{(j)}$. Then, the energetic variational principle implies

$$
\begin{cases}
v_n^{(j)} = \mu \sigma(\Delta^{(j)}\alpha) \kappa^{(j)}, \quad \text{on } \Gamma_t^{(j)}, \ t > 0, \\
\dfrac{d\alpha^{(k)}}{dt} = -\gamma \dfrac{\delta E}{\delta \alpha^{(k)}}, \\
\dfrac{d\boldsymbol{a}^{(l)}}{dt} = \eta \sum_{\boldsymbol{a}^{(l)} \in \Gamma_t^{(j)}} \left(\sigma(\Delta^{(j)}\alpha) \dfrac{\boldsymbol{b}^{(j)}}{|\boldsymbol{b}^{(j)}|} \right), \quad t > 0.
\end{cases}
\tag{6.2}
$$

As in [15], we consider the relaxation parameters, $\mu \to \infty$, and we further assume that the energy density $\sigma(\theta)$ is an even function with respect to the misorientation $\theta = \Delta^{(j)}\alpha$, that is, the misorientation effects are symmetric with respect to the difference

between the lattice orientations. Then, the problem (6.2) becomes,

$$
\begin{cases}
\Gamma_t^{(j)} \text{ is a line segment between some } \boldsymbol{a}^{(l_{j,1})} \text{ and } \boldsymbol{a}^{(l_{j,2})}, \\[2mm]
\dfrac{d\alpha^{(k)}}{dt} = -\gamma \sum_{\substack{\text{grain with } \alpha^{(k')} \text{ is the neighbor of the grain with } \alpha^{(k)} \\ \Gamma_t^{(j)} \text{ is formed by the two grains with } \alpha^{(k)} \text{ and } \alpha^{(k')}}} |\Gamma_t^{(j)}| \sigma_\theta(\alpha^{(k)} - \alpha^{(k')}), \\[2mm]
\dfrac{d\boldsymbol{a}^{(l)}}{dt} = \eta \sum_{\boldsymbol{a}^{(l)} \in \Gamma_t^{(j)}} \left(\sigma(\Delta^{(j)}\alpha) \dfrac{\boldsymbol{b}^{(j)}}{|\boldsymbol{b}^{(j)}|} \right).
\end{cases}
\tag{6.3}
$$

To obtain the global solution of the system (6.3), we assume that there are no critical events in the system (for example, the critical events are disappearance of the grains and/or grain boundaries during coarsening of the system), and we consider an associated energy minimizing state, $(\alpha_\infty^{(k)}, \boldsymbol{a}_\infty^{(l)})$ of (6.3). Then, $(\alpha_\infty^{(k)}, \boldsymbol{a}_\infty^{(l)})$ satisfies,

$$
\begin{cases}
\Gamma_\infty^{(j)} \text{ is a line segment between some } \boldsymbol{a}_\infty^{(l_{j,1})} \text{ and } \boldsymbol{a}_\infty^{(l_{j,2})}, \\[2mm]
0 = -\gamma \sum_{\substack{\text{grain with } \alpha^{(k')} \text{ is the neighbor of the grain with } \alpha^{(k)} \\ \Gamma_t^{(j)} \text{ is formed by the two grains with } \alpha^{(k)} \text{ and } \alpha^{(k')}}} |\Gamma_\infty^{(j)}| \sigma_\theta(\alpha_\infty^{(k)} - \alpha_\infty^{(k')}), \\[2mm]
\boldsymbol{0} = \eta \sum_{\boldsymbol{a}_\infty^{(l)} \in \Gamma_\infty^{(j)}} \left(\sigma(\Delta^{(j)}\alpha_\infty) \dfrac{\boldsymbol{b}_\infty^{(j)}}{|\boldsymbol{b}_\infty^{(j)}|} \right).
\end{cases}
\tag{6.4}
$$

Hence, the total energy E_∞ of the grain boundary network (6.4) is

$$
E_\infty = \sum_j \sigma(\Delta^{(j)}\alpha_\infty) |\boldsymbol{b}_\infty^{(j)}| = \inf \left\{ \sum_j \sigma(\Delta^{(j)}\alpha_\infty) |\boldsymbol{b}^{(j)}| \right\}.
\tag{6.5}
$$

REMARK 6.1.   Note, we assume in (6.3)-(6.4) that the total number of grains, grain boundaries and triple junctions are the same as in the initial configuration (assumption of no critical events in the network).

If there is a neighborhood $U^{(l)} \subset \mathbb{R}^2$ of $\boldsymbol{a}_\infty^{(l)}$ such that

$$
E_\infty < \sum_j |\boldsymbol{b}^{(j)}|
\tag{6.6}
$$

for all $\boldsymbol{a}^{(l)} \in U^{(l)}$, one can obtain a priori estimate for the triple junctions, and, hence, obtain the time-global solution of (6.3). Note that, the assumption (6.6) is related to the boundary condition of the line segments $\Gamma_t^{(j)}$. Further, if the energy minimizing state is unique, then we can proceed with the same argument as in Lemma 4.1, and obtain the global solution (6.3) near the energy minimizing state.

EXAMPLE 6.1.   *Note that, the solution of (6.4) may not be unique even though the grain orientations are constant (misorientation is zero). The total grain boundary energy in the left plot is different from the one in the right plot, see Figure 6.1.*

The asymptotics of the grain boundary networks are rather nontrivial. Our arguments rely on the uniqueness of the equilibrium state (2.9), but we do not know the uniqueness of solutions of the equilibrium state for the grain boundary network (6.4).
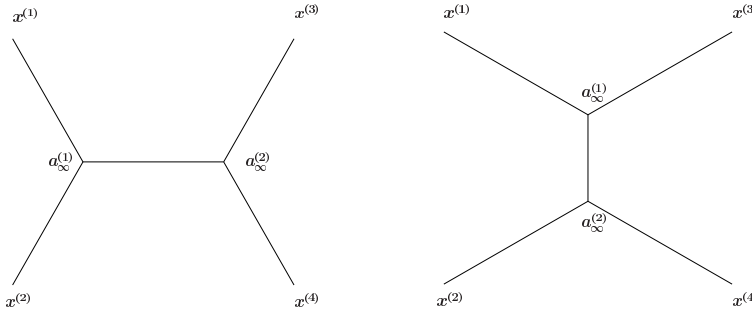
FIG. 6.1. *Even though, there is no misorientation effect, there are at least two equilibrium states for* (6.4).

Thus, in general we cannot take a full limit for the large-time asymptotic behavior. Concluding the above arguments, we have

COROLLARY 6.1.   *In a grain boundary network* (6.3)*, assume that the initial configuration is sufficiently close to an associated energy minimizing state* (6.4)*. Then, there is a global solution* $(\alpha^{(k)}, \boldsymbol{a}^{(l)})$ *of* (6.3)*. Furthermore, there exists a time sequence* $t_n \to \infty$ *such that* $(\alpha^{(k)}(t_n), \boldsymbol{a}^{(l)}(t_n))$ *converges to an associated equilibrium configuration* (6.4).

7. Numerical experiments
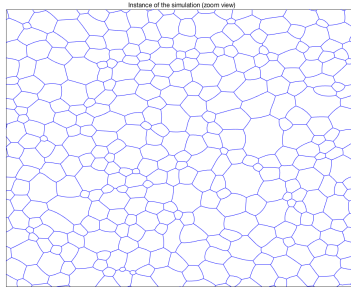
FIG. 7.1. *Time instance from the 2D grain growth simulation with time-dependent orientation (zoom view).*

Here, we present several numerical experiments to illustrate the effects of the dynamic orientations/misorientations (grains "rotations") and of the mobility of the triple junctions, as described in Sections 5-6. In particular, the main goal of our numerical experiments is to illustrate the time scales effect of the mobility of the triple junctions η and the misorientations γ on how the grain boundary system (see Figure 7.1) decays energy and coarsens with time. For that we will study numerically evolution of the total grain boundary energy $E(t)$ (6.1),

$$E(t) = \sum_j \sigma(\Delta^{(j)}\alpha)|\Gamma_t^{(j)}|, \tag{7.1}$$

where as before, $\Delta^{(j)}\alpha$ is a misorientation of the grain boundary $\Gamma^{(j)}$, and $|\Gamma^{(j)}|$ is the length of the grain boundary. We will also consider the growth of the average area,

defined as,

$$A(t) = \frac{4}{N(t)},\tag{7.2}$$

here 4 is the total area of the sample, and $N(t)$ is the total number of grains at time t. The growth of the average area is closely related to the coarsening rate of the grain system that undergoes critical/disappearance events. However, it is important to note that critical events not only include grain disappearance, but also include facet/grain boundary disappearance, facet interchange, splitting of unstable junctions. Further, we will investigate the distribution of the grain boundary character distribution (GBCD) $\rho(\Delta^{(j)}\alpha)$ at T_∞ (T_∞ is defined below). The GBCD (in our context) is an empirical statistical measure of the relative length (in 2D) of the grain boundary interface with a given lattice misorientation,

$$\rho(\Delta^{(j)}\alpha, t) = \text{ relative length of interface of lattice misorientation } \Delta^{(j)}\alpha \text{ at time } t,$$

$$\text{normalized so that } \int_{\Omega_{\Delta^{(j)}\alpha}} \rho d\Delta^{(j)}\alpha = 1,\tag{7.3}$$

where we consider $\Omega_{\Delta^{(j)}\alpha} = [-\frac{\pi}{4}, \frac{\pi}{4}]$ in the numerical experiments below (for planar grain boundary network, it is reasonable to consider such range for the misorientations). For more details, see for example [4]. In all our tests below, we compare GBCD at T_∞ to the stationary solution of the Fokker-Planck equation, the Boltzmann distribution for the grain boundary energy density $\sigma(\Delta^{(j)}\alpha)$,

$$\rho_D(\Delta^{(j)}\alpha) = \frac{1}{Z_D} e^{-\frac{\sigma(\Delta^{(j)}\alpha)}{D}},$$

with partition function, i.e.,normalization factor

$$Z_D = \int_{\Omega_{\Delta^{(j)}\alpha}} e^{-\frac{\sigma(\Delta^{(j)}\alpha)}{D}} d\Delta^{(j)}\alpha,\tag{7.4}$$

[2–5]. We employ Kullback-Leibler relative entropy test to obtain a unique "temperature-like" parameter D and to construct the corresponding Boltzmann distribution for the GBCD at T_∞ as it was originally done in [2–5]. Note, that the GBCD is a primary candidate to characterize texture of the grain boundary network, and is inversely related to the grain boundary energy density as discovered in experiments and simulations. The reader can consult, for example, [2–5] for more details about GBCD and the theory of the GBCD. In the numerical experiments in this paper, we consider the grain boundary energy density as plotted in Figure 7.2 and given below,

$$\sigma(\Delta^{(j)}\alpha) = 1 + 0.25\sin^2(2\Delta^{(j)}\alpha).$$

We consider simulation of 2D grain boundary network using further extension of the algorithm based on sharp interface approach [2, 5] (note, that in [2, 5], only Herring conditions at triple junctions were considered, i.e., $\eta \to \infty$, and dynamic orientations/misorientations ("rotation of grains") was absent, i.e., $\gamma = 0$). We recall that in the numerical scheme we work with a variational principle. The cornerstone of the algorithm, which assures its stability, is the discrete dissipation inequality for the total grain boundary energy that holds when either the discrete Herring boundary condition ($\eta \to \infty$) or discrete "dynamic boundary condition" (finite mobility η of the triple junctions, third equation of (6.2)) is satisfied at the triple junctions. We also recall that

in the numerical algorithm we impose Mullins theory (first equation of (6.2)) as the local evolution law for the grain boundaries (and the time scale μ is kept finite). For more details about computational model based on Mullins equations (curvature driven growth), the reader can consult, for example [2,5].
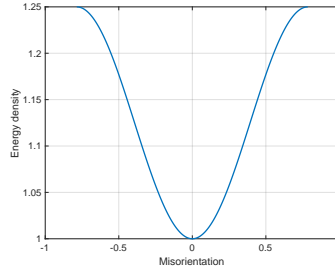

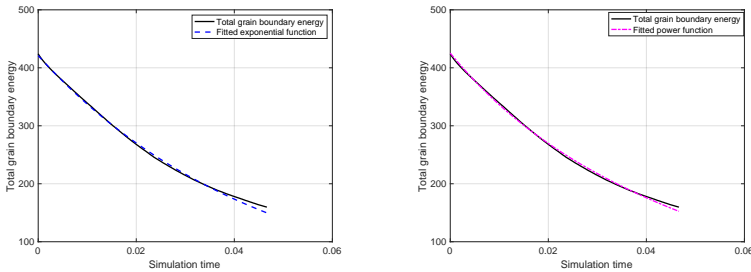FIG. 7.2. *Grain boundary energy density function $\sigma(\Delta\alpha)$.*

FIG. 7.3. *One run of $2D$ trial with 10000 initial grains: (a) Left plot, Total grain boundary energy plot (solid black) versus fitted exponential decaying function $y(t) = 421\exp(-22.16t)$ (dashed blue); (b) Right plot, Total grain boundary energy plot (solid black) versus fitted power law decaying function $y_1(t) = -201.4 + 626.67(1.0 + 16.53t)^{-1}$ (dashed magenta). Mobility of the triple junctions is $\eta = 10$ and the misorientation parameter $\gamma = 1$.*
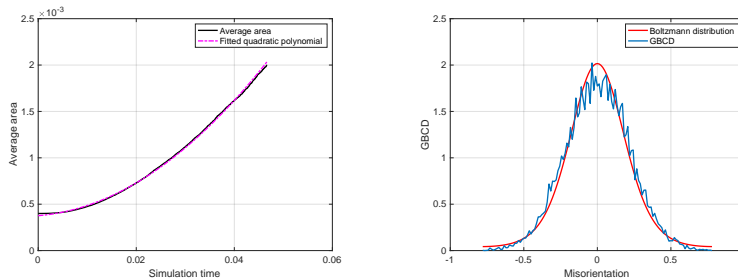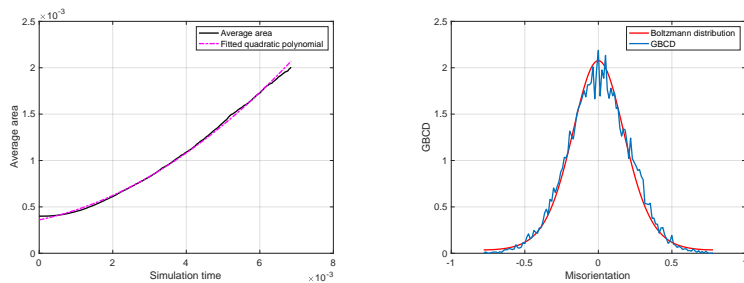

FIG. 7.4. *(a) Left plot, One run of $2D$ trial with 10000 initial grains: Growth of the average area of the grains (solid black) versus fitted quadratic polynomial function $y(t) = 0.6704t^2 + 0.004265t + 0.0003764$ (dashed magenta). (b) Right plot, GBCD at T_∞ (blue curve) averaged over 3 runs of $2D$ trials with 10000 initial grains versus Boltzmann distribution with "temperature"- $D \approx 0.0650$ (red curve). Mobility of triple junctions is $\eta = 10$ and the misorientation parameter $\gamma = 1$.*

In all the numerical tests below we initialized our system with 10^4 cells/grains with normally distributed misorientation angles at initial time $t = 0$. We also assume that the final time of the simulations T_∞ is the time when approximately 80% of grains disappeared from the system, namely the time when only about 2000 cells/grains remain. The final time is selected based on the system with no dynamic misorientations ($\gamma = 0$)
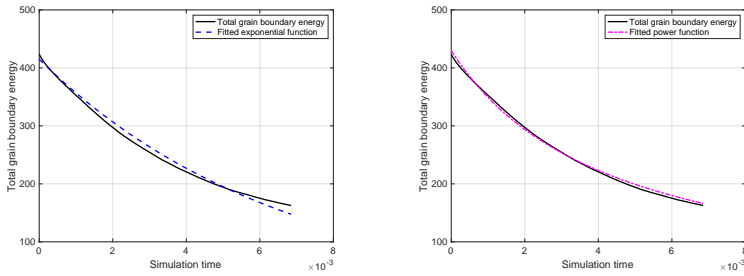
FIG. 7.5. *One run of* $2D$ *trial with* 10000 *initial grains: (a) Left plot, Total grain boundary energy plot (solid black) versus fitted exponential decaying function* $y(t) = 415 \exp(-151t)$ *(dashed blue); (b) Right plot, Total grain boundary energy plot (solid black) versus fitted power law decaying function* $y_1(t) = 429.8286(1.0 + 231.5887t)^{-1}$ *(dashed magenta). Mobility of the triple junctions is* $\eta = 100$ *and the misorientation parameter* $\gamma = 1$.

FIG. 7.6. *(a) Left plot, One run of* $2D$ *trial with* 10000 *initial grains: Growth of the average area of the grains (solid black) versus fitted quadratic polynomial function* $y(t) = 24.34t^2 + 0.083t + 0.00036$ *(dashed magenta). (b) Right plot, GBCD at* T_∞ *(blue curve) averaged over 3 runs of* $2D$ *trials with* 10000 *initial grains versus Boltzmann distribution with "temperature"-* $D \approx 0.0618$ *(red curve). Mobility of triple junctions is* $\eta = 100$ *and the misorientation parameter* $\gamma = 1$.
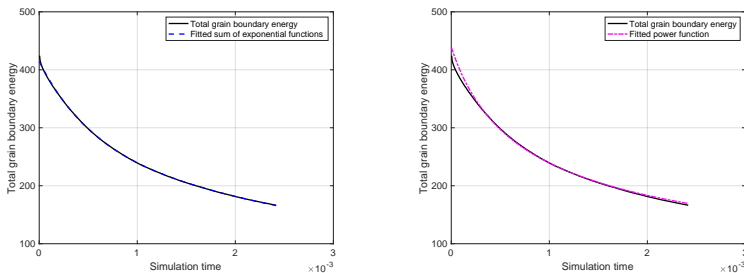
FIG. 7.7. *One run of* $2D$ *trial with* 10000 *initial grains: (a) Left plot, Total grain boundary energy plot (solid black) versus fitted sum of exponential decaying functions* $y(t) = 262.6 \exp(-194.6t) + 151.9 \exp(-1868t)$ *(dashed blue); (b) Right plot, Total grain boundary energy plot (solid black) versus fitted power law decaying function* $y_1(t) = 439.3001(1.0 + 2369.2t)^{-0.5}$ *(dashed magenta). Herring Condition is imposed at the triple junctions* $\eta \to \infty$ *and no "dynamic" misorientation.*

and with Herring condition at the triple junctions ($\eta \to \infty$) and, it is selected to ensure that statistically significant number of grains still remain in the system and the system reached its statistical stead-state. Therefore, all the numerical results which are presented below are for the grain boundary system that undergoes critical/disappearance events.

In the first series of tests, we study the effect of the triple junctions dynamics on the dissipation and coarsening of the system, see Figures 7.3-7.6 (finite mobility η) and
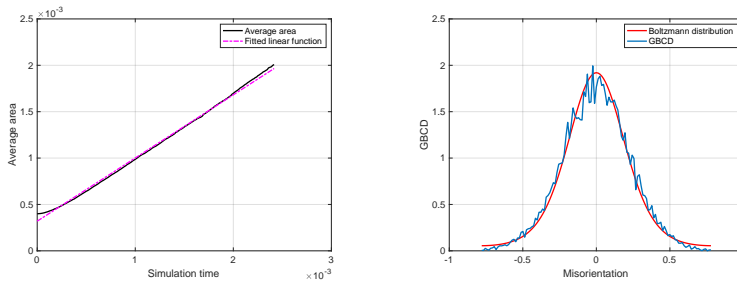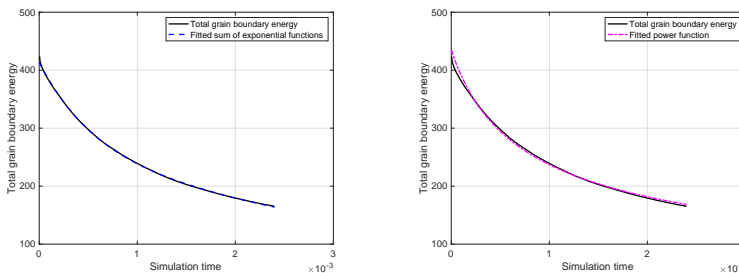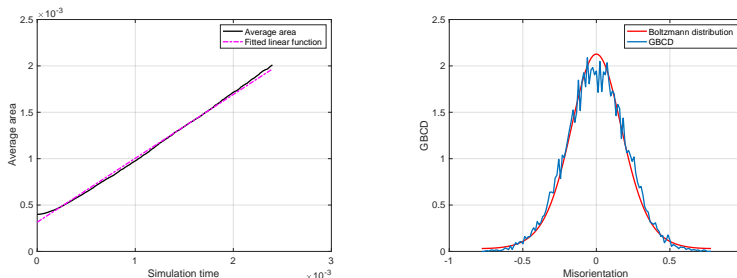
Fig. 7.8. *(a) Left plot, One run of 2D trial with 10000 initial grains: Growth of the average area of the grains (solid black) versus fitted linear function $y(t) = 0.6811t + 0.0003198$ (dashed magenta). (b) Right plot, GBCD at T_∞ (blue curve) averaged over 3 runs of 2D trials with 10000 initial grains versus Boltzmann distribution with "temperature"- $D \approx 0.0704$ (red curve). Herring Condition is imposed at the triple junctions $\eta \to \infty$ and no "dynamic" misorientation.*

Fig. 7.9. *One run of 2D trial with 10000 initial grains: (a) Left plot, Total grain boundary energy plot (solid black) versus fitted sum of exponential decaying functions $y(t) = 263.5 \exp(-202.3t) + 150.3 \exp(-1859t)$ (dashed blue); (b) Right plot, Total grain boundary energy plot (solid black) versus fitted power law decaying function $y_1(t) = 435.3778(1.0 + 2369.2t)^{-0.5}$ (dashed magenta). Herring Condition is imposed at the triple junctions $\eta \to \infty$ and the misorientation parameter $\gamma = 1$.*

Fig. 7.10. *(a) Left plot, One run of 2D trial with 10000 initial grains: Growth of the average area of the grains (solid black) versus fitted linear function $y(t) = 0.6884t + 0.0003154$ (dashed magenta). (b) Right plot, GBCD at T_∞ (blue curve) averaged over 3 runs of 2D trials with 10000 initial grains versus Boltzmann distribution with "temperature"- $D \approx 0.0594$ (red curve). Herring Condition is imposed at the triple junctions $\eta \to \infty$ and the misorientation parameter $\gamma = 1$.*

Figures 7.9-7.10 (Herring condition, $\eta \to \infty$) and misorientation time scale parameter γ is set to 1. We observe that for smaller values of the mobility of the triple junctions η, the energy decay $E(t)$ is well-approximated by an exponential decay, see Figure 7.3 (left plot) which is consistent with the results of our theory, see Section 5 and energy decay (5.34), even though, the theoretical results are obtained under assumption of no critical events and $\mu \to \infty$. In comparison, we also present fit to a power law decaying function, see Figure 7.3 (right plot). The power law function does not seem to give
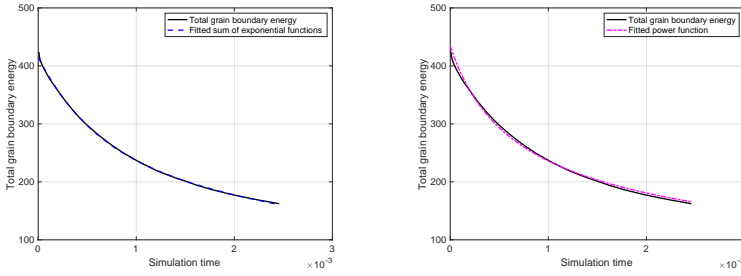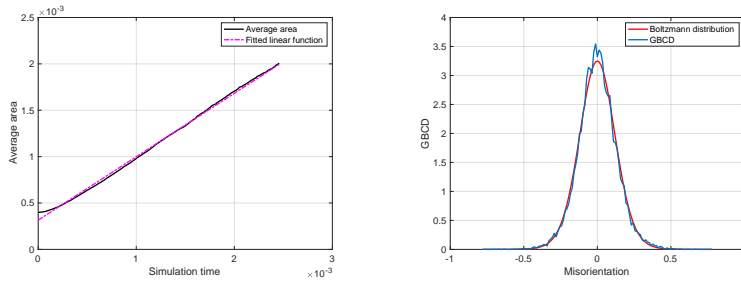
FIG. 7.11. *One run of* 2D *trial with* 10000 *initial grains: (a) Left plot, Total grain boundary energy plot (solid black) versus fitted sum of exponential decaying functions* $y(t) = 248 \exp(-182.8t) + 166.8 \exp(-1708t)$ *(dashed blue); (b) Right plot, Total grain boundary energy plot (solid black) versus fitted power law decaying function* $y_1(t) = 434.6254(1.0 + 2388.1t)^{-0.5}$ *(dashed magenta). Herring Condition is imposed at the triple junctions* $\eta \to \infty$ *and the misorientation parameter* $\gamma = 1000$.

FIG. 7.12. *(a) Left plot, One run of* 2D *trial with* 10000 *initial grains: Growth of the average area of the grains (solid black) versus fitted linear function* $y(t) = 0.6834t + 0.0003155$ *(dashed magenta). (b) Right plot, GBCD at* T_∞ *(blue curve) averaged over 3 runs of* 2D *trials with* 10000 *initial grains versus Boltzmann distribution with "temperature"-* $D \approx 0.0283$ *(red curve). Herring Condition is imposed at the triple junctions* $\eta \to \infty$ *and the misorientation parameter* $\gamma = 1000$.

as good approximation in this case, due to the appearance of the negative term in the fitted power function. However, for larger values of η, Figure 7.5 (left plot) and for Herring condition ($\eta \to \infty$), Figure 7.9 (see also Figures 7.7 and 7.11 with different values of γ) (left plots), we obtain that the total grain boundary energy does not follow exponential decay, and the sum of exponential functions or power law functions give better description of the energy decay, see Figure 7.9 (see also Figures 7.7 and 7.11 with different values of γ). Note also, that the numerically observed energy decay rates increase with the mobility η of the triple junctions which is also consistent with the developed theory, see Sections 5-6. In addition, we observe that the average area grows as quadratic function in time for the finite mobility η of the triple junctions, Figures 7.4 and 7.6 (left plots) but it exhibits a linear growth with $\eta \to \infty$, Herring condition at the triple junctions, Figure 7.10 (see also Figures 7.8 and 7.12 with different values of γ) (left plots). We also observe that the coarsening rate of grain systems slows down with the smaller η, see Figures 7.4, 7.6, 7.10 for the growth of the average area (see also Figures 7.8 and 7.12 with different values of γ) (left plots). The observations about the growth of the average area and the coarsening rate can be explained by noting that with Herring condition at the triple junctions ($\eta \to \infty$), the grain growth is driven mainly by the kinetics of grain boundaries, but not the triple junctions. And, the von Neumann-Mullins $n-6$ rule for the area of n-sided grain is satisfied approximately (due to anisotropy) in that case. With the finite mobility η of the triple junctions, triple

junctions dynamics play an important role in the grain growth. Hence, finite mobility of the triple junctions can result in the growth of "smaller" grains (with sides less than 6) and, at the same time, it can result in the disappearance of the "larger" grains (with sides greater than 6), namely, the von Neumann-Mullins $n-6$ rule will not be valid in the same way anymore. We also note that the energy decay in our numerical tests is consistent with the growth of the average area. Moreover, we observe that dynamics of the triple junctions show some effect on the GBCD at T_∞, in particular, slight decrease in the diffusion coefficient/ in the "temperature" like parameter D with increase of η, but not a significant change, Figures 7.4, 7.6 and 7.10 (right plots), (note, the "temperature" like parameter D accounts for various critical events–grains disappearance, facet/grain boundary disappearance, facet interchange, splitting of unstable junctions).

For the other series of tests, we impose Herring condition at the triple junctions ($\eta \to \infty$), but we vary the misorientation parameter γ, second equation of (6.2). We do not observe as much effect on the energy decay or average area growth in this case (probably due to the effect of the Herring condition at the triple junctions), but we observe the significant effect on the GBCD at T_∞ and the diffusion coefficient/"temperature"-like parameter D, see Figures 7.7-7.12. As concluded from our numerical results, larger values of γ give smaller diffusion coefficient/"temperature"-like parameter D, and hence higher GBCD peak near misorientation 0. This is consistent with our theory that basically, larger misorientation parameter γ produces direct motion of misorientations towards equilibrium state of zero misorientations, see Section 2 and also [15]. Furthermore, from all numerical experiments with dynamic misorientation and with different triple junction mobilities, we observe that the GBCD at T_∞ is well-approximated by the Boltzmann distribution for the grain boundary energy density, see Figures 7.4, 7.6, 7.8, 7.10 and 7.12 (right plots), which is similar to the work in [2–5], but more detailed analysis needs to be done for a system that undergoes critical events to understand the relation between GBCD, "temperature"-like/diffusion parameter D, and different relaxation time scales, as well as the effect of the time scales on the dissipation mechanism and certain coarsening rates.

REMARK 7.1.   Note that, we performed 3 runs for each numerical test presented in this work. We report results of a single run for the energy decay and the growth of the average area (the results from the other two runs for each test were very similar to the presented ones), and we illustrate, averaged over the 3 runs, the GBCD statistics at T_∞. The curve-fitting for the energy and the average area plots was done using Matlab [29] toolbox cftool.

REMARK 7.2.   Note, that the proposed model of dynamic orientations (6.2) (and, hence, dynamic misorientations), or Langevin-type equation if critical events/disappearance events are taken into account is reminiscent of the recently developed theory for the grain boundary character distribution (GBCD) [2–5], which suggests that the evolution of the GBCD satisfies a Fokker-Planck equation. More details will be presented in future studies.

Appendix. Explicit form of the decay rate of the linearized problem (5.7). In this appendix, we give an explicit form of the constant λ_2, which is a minimum eigenvalue of

$$L_{\boldsymbol{a}} = \sum_{j=1}^{3} \frac{1}{|\boldsymbol{b}_\infty^{(j)}|} \left(I - \frac{\boldsymbol{b}_\infty^{(j)}}{|\boldsymbol{b}_\infty^{(j)}|} \otimes \frac{\boldsymbol{b}_\infty^{(j)}}{|\boldsymbol{b}_\infty^{(j)}|} \right).$$

Since $L_{\boldsymbol{a}}$ is a two-dimensional matrix, it is enough to manipulate the trace and the determinant of $L_{\boldsymbol{a}}$. The trace of $L_{\boldsymbol{a}}$ is easily calculated as

$$\operatorname{tr} L_{\boldsymbol{a}} = \sum_{j=1}^{3} \frac{1}{|\boldsymbol{b}_\infty^{(j)}|} \left(2 - \operatorname{tr} \frac{\boldsymbol{b}_\infty^{(j)}}{|\boldsymbol{b}_\infty^{(j)}|} \otimes \frac{\boldsymbol{b}_\infty^{(j)}}{|\boldsymbol{b}_\infty^{(j)}|} \right) = \sum_{j=1}^{3} \frac{1}{|\boldsymbol{b}_\infty^{(j)}|}.$$

Next we consider the determinant of $L_{\boldsymbol{a}}$. Denote $\boldsymbol{b}_\infty^{(j)} = (b_{\infty,1}^{(j)}, b_{\infty,2}^{(j)})$, $b_k^{(j)} := \frac{b_{\infty,k}^{(j)}}{b_\infty^{(j)}}$, and $b_\infty^{(j)} = |\boldsymbol{b}_\infty^{(j)}|$. Then,

$$L_{\boldsymbol{a}} = \sum_{j=1}^{3} \begin{pmatrix} \frac{1}{b_\infty^{(j)}} \left(1 - \left(b_1^{(j)} \right)^2 \right) & -\frac{1}{b_\infty^{(j)}} b_1^{(j)} b_2^{(j)} \\ -\frac{1}{b_\infty^{(j)}} b_1^{(j)} b_2^{(j)} & \frac{1}{b_\infty^{(j)}} \left(1 - \left(b_2^{(j)} \right)^2 \right) \end{pmatrix}$$

hence,

$$
\begin{aligned}
\det L_{\boldsymbol{a}} &= \left(\sum_{j=1}^{3} \frac{1}{b_\infty^{(j)}} \left(1 - \left(b_1^{(j)} \right)^2 \right) \right) \left(\sum_{j=1}^{3} \frac{1}{b_\infty^{(j)}} \left(1 - \left(b_2^{(j)} \right)^2 \right) \right) - \left(\sum_{j=1}^{3} \frac{1}{b_\infty^{(j)}} b_1^{(j)} b_2^{(j)} \right)^2 \\
&= \sum_{j=1}^{3} \frac{1}{(b_\infty^{(j)})^2} \left(\left(1 - \left(b_1^{(j)} \right)^2 \right) \left(1 - \left(b_2^{(j)} \right)^2 \right) - \left(b_1^{(j)} b_2^{(j)} \right)^2 \right) \\
&\quad + \sum_{j \neq k} \frac{1}{b_\infty^{(j)}} \frac{1}{b_\infty^{(k)}} \left(\left(1 - \left(b_1^{(j)} \right)^2 \right) \left(1 - \left(b_2^{(k)} \right)^2 \right) - \left(b_1^{(j)} b_2^{(j)} \right) \left(b_1^{(k)} b_2^{(k)} \right) \right) \\
&= \sum_{j \neq k} \frac{1}{b_\infty^{(j)}} \frac{1}{b_\infty^{(k)}} \left(\left(1 - \left(b_1^{(j)} \right)^2 \right) \left(1 - \left(b_2^{(k)} \right)^2 \right) - \left(b_1^{(j)} b_2^{(j)} \right) \left(b_1^{(k)} b_2^{(k)} \right) \right) \\
&= \sum_{j < k} \frac{1}{b_\infty^{(j)}} \frac{1}{b_\infty^{(k)}} \left(1 - \left(b_1^{(j)} \right)^2 - \left(b_2^{(k)} \right)^2 + \left(b_1^{(j)} \right)^2 \left(b_2^{(k)} \right)^2 \right. \\
&\quad \left. + 1 - \left(b_1^{(k)} \right)^2 - \left(b_2^{(j)} \right)^2 + \left(b_1^{(k)} \right)^2 \left(b_2^{(j)} \right)^2 - 2 \left(b_1^{(j)} b_2^{(j)} b_1^{(k)} b_2^{(k)} \right) \right) \\
&= \sum_{j < k} \frac{1}{b_\infty^{(j)}} \frac{1}{b_\infty^{(k)}} \left(b_1^{(j)} b_2^{(k)} - b_2^{(j)} b_1^{(k)} \right)^2 = \sum_{j < k} \frac{1}{b_\infty^{(j)}} \frac{1}{b_\infty^{(k)}} \left(\frac{\boldsymbol{b}_\infty^{(j)}}{|\boldsymbol{b}_\infty^{(j)}|} \cdot R_{-\frac{\pi}{2}} \frac{\boldsymbol{b}_\infty^{(k)}}{|\boldsymbol{b}_\infty^{(k)}|} \right)^2,
\end{aligned}
$$

where $R_{-\frac{\pi}{2}} = \begin{pmatrix} 0 & 1 \\ -1 & 0 \end{pmatrix}$ is the $-\frac{\pi}{2}$ rotating matrix, and note that $(b_1^{(j)})^2 + (b_2^{(j)})^2 = 1$. We also know that, $\left\{ \frac{\boldsymbol{b}_\infty^{(k)}}{|\boldsymbol{b}_\infty^{(k)}|}, \ R_{-\frac{\pi}{2}} \frac{\boldsymbol{b}_\infty^{(k)}}{|\boldsymbol{b}_\infty^{(k)}|} \right\}$ is orthonormal basis on $\mathbb{R}^2$. Thus for $1 \leq j, k \leq 3$, by Parseval's identity tells us

$$\left(\frac{\boldsymbol{b}_\infty^{(j)}}{|\boldsymbol{b}_\infty^{(j)}|} \cdot \frac{\boldsymbol{b}_\infty^{(k)}}{|\boldsymbol{b}_\infty^{(k)}|} \right)^2 + \left(\frac{\boldsymbol{b}_\infty^{(j)}}{|\boldsymbol{b}_\infty^{(j)}|} \cdot R_{-\frac{\pi}{2}} \frac{\boldsymbol{b}_\infty^{(k)}}{|\boldsymbol{b}_\infty^{(k)}|} \right)^2 = 1.$$

Since,

$$\frac{\boldsymbol{b}_\infty^{(j)}}{|\boldsymbol{b}_\infty^{(j)}|} \cdot \frac{\boldsymbol{b}_\infty^{(k)}}{|\boldsymbol{b}_\infty^{(k)}|} = -\frac{1}{2} + \frac{3}{2} \delta_{jk},$$

we finally arrive, for $j \neq k$

$$\left(\frac{\boldsymbol{b}_\infty^{(j)}}{|\boldsymbol{b}_\infty^{(j)}|} \cdot R_{-\frac{\pi}{2}} \frac{\boldsymbol{b}_\infty^{(k)}}{|\boldsymbol{b}_\infty^{(k)}|} \right)^2 = \frac{3}{4}.$$

Then $\lambda_2 > 0$ in Lemma 5.2 is explicitly given by,

$$\begin{aligned}
\lambda_2 &= \frac{1}{2} \left(\mathrm{tr}\, L_{\boldsymbol{a}} - \sqrt{(\mathrm{tr}\, L_{\boldsymbol{a}})^2 - 4(\det L_{\boldsymbol{a}})} \right) \\
&= \frac{1}{2} \left(\sum_{j=1}^3 \frac{1}{|\boldsymbol{b}_\infty^{(j)}|} - \sqrt{\left(\sum_{j=1}^3 \frac{1}{|\boldsymbol{b}_\infty^{(j)}|} \right)^2 - 3 \left(\sum_{j<k} \frac{1}{|\boldsymbol{b}_\infty^{(j)}|} \frac{1}{|\boldsymbol{b}_\infty^{(k)}|} \right)} \right) \\
&= \frac{1}{2} \left(\sum_{j=1}^3 \frac{1}{|\boldsymbol{b}_\infty^{(j)}|} - \sqrt{\frac{1}{2} \sum_{j<k} \left(\frac{1}{|\boldsymbol{b}_\infty^{(j)}|} - \frac{1}{|\boldsymbol{b}_\infty^{(k)}|} \right)^2} \right).
\end{aligned} \tag{7.5}$$

REFERENCES

[1] H. Abels, H. Garcke, and L. Müller, *Stability of spherical caps under the volume-preserving mean curvature flow with line tension*, Nonlinear Anal., 117:8–37, 2015. 1

[2] P. Bardsley, K. Barmak, E. Eggeling, Y. Epshteyn, D. Kinderlehrer, and S. Ta'asan, *Towards a gradient flow for microstructure*, Atti Accad. Naz. Lincei Cl. Sci. Fis. Mat. Natur., 28(4):777–805, 2017. 1, 2, 7, 7, 7.2

[3] K. Barmak, E. Eggeling, M. Emelianenko, Y. Epshteyn, D. Kinderlehrer, and S. Ta'asan, *Geometric growth and character development in large metastable networks*, Rend. Mat. Appl.(7), 29(1):65–81, 2009. 1, 2, 7, 7, 7.2

[4] K. Barmak, E. Eggeling, M. Emelianenko, Y. Epshteyn, D. Kinderlehrer, R. Sharp, and S. Ta'asan, *Critical events, entropy, and the grain boundary character distribution*, Phys. Rev. B, 83:134117, 2011. 1, 2, 7, 7, 7, 7.2

[5] K. Barmak, E. Eggeling, M. Emelianenko, Y. Epshteyn, D. Kinderlehrer, R. Sharp, and S. Ta'asan, *An entropy based theory of the grain boundary character distribution*, Discrete Contin. Dyn. Syst., 30:427–454, 2011. 1, 2, 7, 7, 7.2

[6] K. Barmak, E. Eggeling, D. Kinderlehrer, R. Sharp, S. Ta'asan, A.D. Rollett, and K.R. Coffey, *Grain growth and the puzzle of its stagnation in thin films: The curious tale of a tail and an ear*, Prog. Mater. Sci., 58:987–1055, 2013. 1

[7] V. Boltyanski, H. Martini, and V. Soltan, *Geometric Methods and Optimization Problems*, Combinatorial Optimization, Kluwer Academic Publishers, Dordrecht, 4, 1999. 5

[8] K.A. Brakke, *The Motion of a Surface by its Mean Curvature*, Princeton University Press, 1978. 1

[9] L. Bronsard and F. Reitich, *On three-phase boundary motion and the singular limit of a vector-valued Ginzburg-Landau equation*, Arch. Ration. Mech. Anal., 124:355–379, 1993. 1

[10] Y.G. Chen, Y. Giga, and S. Goto, *Uniqueness and existence of viscosity solutions of generalized mean curvature flow equations*, J. Diff. Geom., 33:749–786, 1991. 1

[11] K. Ecker, *Regularity Theory for Mean Curvature Flow*, Progress in Nonlinear Differential Equations and Their Applications, Birkhäuser, 2004. 1

[12] M. Elsey and S. Esedoḡlu, *Threshold dynamics for anisotropic surface energies*, Math. Comput., 87(312):1721–1756, 2018. 1

[13] M. Elsey, S. Esedoḡlu, and P. Smereka, *Diffusion generated motion for grain growth in two and three dimensions*, J. Comput. Phys., 228(21):8015–8033, 2009. 1

[14] M. Elsey, S. Esedoḡlu, and P. Smereka, *Large-scale simulation of normal grain growth via diffusion-generated motion*, Proc. R. Soc. Lond. Ser. A Math. Phys. Eng. Sci., 467(2126):381–401, 2011. 1

[15] Y. Epshteyn, C. Liu, and M. Mizuno, *Motion of grain boundaries with dynamic lattice misorientations and with triple junctions drag*, SIAM J. Math. Anal., 53(3):3072–3097, 2021. 1, 2, 2, 2, 2.1, 3, 3.1, 3, 3.2, 3.3, 3, 6, 6, 7

[16] L.C. Evans and J. Spruck, *Motion of level sets by mean curvature I*, J. Diff. Geom., 33:635–681, 1991. 1

[17] H. Garcke, Y. Kohsaka, and D. Ševčovič, *Nonlinear stability of stationary solutions for curvature flow with triple function*, Hokkaido Math. J., 38:721–769, 2009. 1

[18] C. Herring, *Surface tension as a motivation for sintering*, in J.M. Ball, D. Kinderlehrer, P. Podio-Guidugli and M. Slemrod (eds.), Fundamental Contributions to the Continuum Theory of Evolving Phase Interfaces in Solids, Springer, 33–69, 1999. 1

[19] L. Kim and Y. Tonegawa, *On the mean curvature flow of grain boundaries*, Ann. Inst. Fourier (Grenoble), 67:43–142, 2017. 1

[20] D. Kinderlehrer and C. Liu, *Evolution of grain boundaries*, Math. Model. Meth. Appl. Sci., 11:713–729, 2001. 1

[21] D. Kinderlehrer, I. Livshits, and S. Ta'asan, *A variational approach to modeling and simulation of grain growth*, SIAM J. Sci. Comput., 28:1694–1715, 2006. 1

[22] R.V. Kohn, *Irreversibility and the statistics of grain boundaries*, Physics, 4:33, 2011. 1

[23] A. Magni, C. Mantegazza, and M. Novaga, *Motion by curvature of planar networks, II*, Ann. Sc. Norm. Super. Pisa Cl. Sci. (5), 15:117–144, 2016. 1

[24] C. Mantegazza, *Lecture Notes on Mean Curvature Flow*, Progress in Mathematics, Birkhäuser, 290, 2011. 1

[25] C. Mantegazza, *Evolution by curvature of networks of curves in the plane*, in P. Baird, A. Fardoun, R. Regbaoui and A. El Soufi (eds.), Variational Problems in Riemannian Geometry, Progr. Nonlinear Diff. Eqs. Appl., Springer, 59:95–109, 2014. 1

[26] C. Mantegazza, M. Novaga, and A. Pluda, *Motion by curvature of networks with two triple junctions*, Geom. Flows, 2:18–48, 2016. 1

[27] C. Mantegazza, M. Novaga, A. Pluda, and F. Schulze, *Evolution of networks with multiple junctions*, arXiv preprint, arXiv:1611.08254. 1

[28] C. Mantegazza, M. Novaga, and V.M. Tortorelli, *Motion by curvature of planar networks*, Ann. Sc. Norm. Super. Pisa Cl. Sci. (5), 3:235–324, 2004. 1

[29] *MATLAB. Version 9.4.0 (R2018a)*, The MathWorks Inc., Natick, Massachusetts, 2018. 7.1

[30] W.W. Mullins, *Two-dimensional motion of idealized grain boundaries*, J. Appl. Phy., 27:900–904, 1956. 1

[31] W.W. Mullins, *Theory of thermal grooving*, J. Appl. Phy., 28:333–339, 1957. 1

[32] S.L. Thomas, C. Wei, J. Han, Y. Xiang, and D.J. Srolovitz, *Disconnection description of triple-junction motion*, Proc. Natl. Acad. Sci. USA, 116:8756–8765, 2019. 1

[33] M. Upmanyu, D.J. Srolovitz, L.S. Shvindlerman, and G. Gottstein, *Triple junction mobility: A molecular dynamics study*, Interface Sci., 7:307–319, 1999. 1

[34] M. Upmanyu, D.J. Srolovitz, L.S. Shvindlerman, and G. Gottstein, *Molecular dynamics simulation of triple junction migration*, Acta Mater., 50:1405–1420, 2002. 1

[35] L. Zhang, J. Han, Y. Xiang, and D.J. Srolovitz, *Equation of motion for a grain boundary*, Phys. Rev. Lett., 119:246101, 2017. 1

[36] L. Zhang and Y. Xiang, *Motion of grain boundaries incorporating dislocation structure*, J. Mech. Phys. Solids, 117:157–178, 2018. 1